

# Thermal conduction by dark matter with velocity and momentum-dependent cross-sections

Aaron C. Vincent\*

*Instituto de Física Corpuscular (IFIC), CSIC-Universitat de València,  
Apartado de Correos 22085, E-46071 Valencia, Spain*

Pat Scott†

*Department of Physics, McGill University 3600 Rue University, Montréal, Québec, Canada H3A 2T8*

We use the formalism of Gould and Raffelt [1] to compute the dimensionless thermal conduction coefficients for scattering of dark matter particles with standard model nucleons via cross-sections that depend on the relative velocity or momentum exchanged between particles. Motivated by models invoked to reconcile various recent results in direct detection, we explicitly compute the conduction coefficients  $\alpha$  and  $\kappa$  for cross-sections that go as  $v_{\text{rel}}^2$ ,  $v_{\text{rel}}^4$ ,  $v_{\text{rel}}^{-2}$ ,  $q^2$ ,  $q^4$  and  $q^{-2}$ , where  $v_{\text{rel}}$  is the relative DM-nucleus velocity and  $q$  is the momentum transferred in the collision. We find that a  $v_{\text{rel}}^{-2}$  dependence can significantly enhance energy transport from the inner solar core to the outer core. The same can true for any  $q$ -dependent coupling, if the dark matter mass lies within some specific range for each coupling. This effect can complement direct searches for dark matter; combining these results with state-of-the-art Solar simulations should greatly increase sensitivity to certain DM models. It also seems possible that the so-called Solar Abundance Problem could be resolved by enhanced energy transport in the solar core due to such velocity- or momentum-dependent scatterings.

## I. INTRODUCTION

If cosmological dark matter (DM) is similar in character to a WIMP (weakly-interacting massive particle), it may possess a weak-scale cross-section for interaction with ordinary nucleons. In this case, collisions between DM particles in the halo of the Milky Way and nuclei in the Sun will slow some of the DM enough to gravitationally bind it to the Sun [2–4]. If enough is captured and remains in the Sun, DM may impact the structure and evolution of the Sun itself [5–7].

The effects of captured DM particles on the Sun and other stars have been a subject of investigation for many decades. Much work has concentrated on the detectable signals of annihilating DM in stellar cores, such as  $\sim$ GeV-scale neutrinos escaping from the Sun [3, 8–22] and the effects of core heating by annihilation products [23–34]. The weakly-interacting nature of WIMP-like DM<sup>1</sup> can also make it a medium for energy transport in the Sun or other stars [5–7], the implications of which have been studied extensively [35–47]. Even when that energy transport is highly localised (i.e. conductive), WIMPs may cool the core by absorbing heat, which can then be deposited at larger radii. These changes can be poten-

tially constrained with the temperature-sensitive <sup>8</sup>B neutrino flux, as well as precision helio/asteroseismological measurements of the sound speed, small frequency separations and gravity modes [48–56].

So far all studies of energy transport by DM particles have assumed that the cross-section for scattering between WIMPs and nuclei is independent of their relative velocity and the momentum exchanged in the collision. This is not because interesting DM models do not exist with velocity or momentum-dependent couplings to nucleons, but simply because the required theoretical background for including their effects in stellar structure simulations does not exist in the literature. Here we provide such calculations for a range of non-constant cross-sections. This work will allow the full transport theory to be incorporated into a solar evolution code that also treats the capture and annihilation of DM, in order to derive self-consistent limits on DM models with non-standard cross-sections.

Our other motivation is the well-known Solar Abundance Problem: recent photospheric analyses [57–65] indicate that the solar metallicity is 10–20% lower than previously thought, putting predictions of solar evolution models computed with the improved photospheric abundances at stark odds with sound-speed profiles inferred from helioseismology [66–71]. A deal of effort has been devoted to finding solutions to this quandary [51–53, 72–81], but so far no proposal has really proven viable. One might postulate that the discrepancy is caused by enhanced energy transport in the solar core mediated by non-standard WIMP-nucleon couplings; the calculations we carry out here allow this proposition to be tested.

This paper is structured as follows: first, in Section II we provide some background on WIMP-nucleon couplings and how one goes about calculating energy trans-

\* [vincent@ific.uv.es](mailto:vincent@ific.uv.es)

† [patscott@physics.mcgill.ca](mailto:patscott@physics.mcgill.ca)

<sup>1</sup> Strictly, the WIMP paradigm implies certain weak-scale annihilation and nuclear scattering cross-sections, a GeV–TeV scale mass and a corresponding natural reproduction of the observed relic density via thermal production. Here all that is important is the interaction with nucleons, so throughout this paper we use ‘WIMP’ loosely to refer to any DM with the requisite nuclear interaction, regardless of its mass or annihilation cross-section.

port by WIMPs, introducing the thermal conduction coefficients  $\alpha$  and  $\kappa$ . In Section III we briefly summarise the relevant equations from Ref. [1] that allow calculation of  $\alpha$  and  $\kappa$ . In Section IV we modify this treatment to account for non-trivial velocity and momentum structure in the scattering cross-section, and show the effect on  $\alpha$  and  $\kappa$ . In Section V we provide some examples of the effect on energy transport in the Sun, then finish with some discussion and concluding remarks in Section VI.

## II. PRELIMINARY THEORY

The quantity that describes microscopic interactions between WIMPs and Standard Model nuclei is the total cross-section  $\sigma$  for WIMP-nucleon scattering. Determining the impacts of energy conduction by a population of weakly-interacting particles in a star means working out their influence on bulk stellar properties like the radial temperature, density and pressure profiles. The established approach to this problem is to solve the Boltzmann collision equation (BCE) inside the spherically symmetric potential well of a star. The formalism and a general solution for standard WIMP-quark couplings were described by Gould and Raffelt [1]. There are three quantities that, together, are sufficient to describe the transport of energy by a diffuse, weakly-interacting massive particle  $\chi$  in a dense medium such as a star:

- $l_\chi$ , defined as the inverse of the mean number of WIMP-nucleon interactions per unit length; this gives the typical distance travelled by a WIMP between scatterings;
- $\alpha$ , related to the thermal diffusion coefficient; this parameterises the efficiency of a species' diffusion inside the potential well;
- $\kappa$ , the dimensionless thermal conduction coefficient; this describes the efficiency of energy transfer from layer to layer in the star.

Given a form of the WIMP-nucleon cross-section  $\sigma$  as a function of the microscopic kinetic variables ( $v_{\text{rel}}$ ,  $q$ , etc.), the coefficients  $\alpha$  and  $\kappa$  are quantities that are averaged over the kinetic gas distributions, thus depending only on  $\mu$ , the ratio between the WIMP mass and the mass of the nucleus with which it scatters. They can therefore be computed once and for all for each type of WIMP-nucleon coupling.

In the following sections, we compute the thermal conduction coefficients  $\alpha$  and  $\kappa$  of WIMPs with non-standard couplings to the standard model, going beyond the  $\sigma = \text{const.}$  case computed explicitly by Ref. [1]. Because these computations must be done on a case by case basis, here we focus on the specific velocity- and momentum-dependent cross-sections  $\sigma \propto v_{\text{rel}}^{2n}$  and

$\sigma \propto q^{2n}$ , with  $n = \{-1, 1, 2\}$ .<sup>2</sup> Here  $v_{\text{rel}}$  is the WIMP-nucleus relative velocity, and  $q$  is the momentum transferred during a collision. Our choice of these types of couplings is motivated in part by a number of recent direct-detection experiments [82–85], but they can easily occur theoretically [86, 87]. Mixed couplings (whether linear combinations of these couplings or cross-terms between them) also each require explicit calculation, and cannot be treated using combinations of the results we present here; we leave these for future work.

The dominant operators which arise in the most basic models of interactions between WIMPs  $\chi$  and standard model particles (namely quarks, denoted  $Q$ ) are  $O_{SI} = \bar{\chi}\chi\bar{Q}Q$  and  $O_{SD} = \bar{\chi}\gamma_\mu\gamma_5\chi\bar{Q}\gamma_\mu\gamma_5Q$ . These respectively lead to the regular spin-independent  $\sigma_{SI}$  and spin-dependent  $\sigma_{SD}$  cross-sections, which have no velocity or momentum structure beyond standard kinematic factors, and have been the focus of exclusion efforts in direct experimental searches to date. Among these, DAMA [82], CoGeNT [83], CRESST-II [84] and CDMS II [85] have reported excess events above their expected backgrounds, consistent with recoils caused by WIMP-like dark matter. On the other hand, LUX [88], XENON10 [89], XENON100 [90], COUPP [91], SIMPLE [92], Super-Kamiokande [19] and IceCube [22], under the assumption of constant scattering cross-sections and a standard halo model, would together exclude such “detections” from being observations of WIMPs. However, there are certain assumptions that are built into the exclusions quoted by such experiments. Although some recent work (e.g. [93, 94]) has focused on the astrophysical uncertainties, other authors have proposed reconciling direct detection results using scattering cross-sections with a non-trivial dependence upon the relative velocity or momentum transfer of the collision [95–104].

Indeed, there is no guarantee that the dominant coupling between the dark sector and the SM is as simple as  $O_{SI}$  or  $O_{SD}$ . Possibilities include a finite particle radius (the dark sector analogue of the nuclear form factor), a vector coupling to quarks, parity-violating interactions such as  $\bar{\chi}\gamma_5\chi\bar{Q}Q$  or  $\bar{\chi}\gamma_\mu\gamma_5\chi\bar{Q}\gamma_\mu\gamma_5Q$  or even a small dipole or anapole interaction with the standard model [96–98, 101–107]. If these terms dominate, then the interaction cross-section will be proportional to some power of the momentum transfer  $q$ :

$$\sigma = \sigma_0 \left( \frac{q}{q_0} \right)^{2n}, \quad (1)$$

where  $\sigma_0$  is the cross-section at some normalisation momentum  $q_0$ . Models charged under multiple gauge fields can display interactions that go as a sum of different powers of  $q^2$  [96]. Even for scattering via standard  $O_{SI}$  or

<sup>2</sup> We do not consider cases where  $n \leq -2$ , as this causes the total momentum transfer to diverge; conduction properties would then intrinsically depend on the chosen cutoff scale.

$O_{SD}$  couplings, scattering between WIMPs and nuclei can be strongly momentum-dependent due to the nuclear form factor. This is especially important at high momentum transfer, so has a large impact on rates at which WIMPs can be scattered to below the local escape velocity and captured by a star. In this paper we neglect the influence of nuclear form factors, mainly because the majority of WIMP scattering in stellar interiors is with hydrogen and helium, at much lower momentum transfer than successful capture events. In the cases where momentum is exchanged with heavier nuclei (mainly C, N and O), the suppression due to a Helm form factor is only a few percent at relevant values of  $q$  – but the form factors should in principle be taken into account if the impact of a given WIMP on a particular star is to be calculated in its fullest, goriest detail.

Operators also exist which produce interactions that depend on the relative velocity  $v_{\text{rel}}$  between the WIMP and the nucleus:

$$\sigma = \sigma_0 \left( \frac{v_{\text{rel}}}{v_0} \right)^{2n}. \quad (2)$$

For instance, cancellations can lead to a p-wave-suppressed cross-section, i.e.  $\sigma \propto v_{\text{rel}}^2$ , whereas a Sommerfeld-like enhancement (an attractive force with a massive carrier) can display “resonant” behaviour, with an enhancement proportional to  $v_{\text{rel}}^{-2}$  [108–110].

Given a certain WIMP mass, a good choice for the reference velocity  $v_0$  in a star is the temperature-dependent velocity

$$v_T(m_\chi, r) = [2k_B T(r)/m_\chi]^{1/2}. \quad (3)$$

The typical thermal WIMP velocity can be obtained by multiplying  $v_T$  by a further factor of  $(3/2)^{1/2}$  [1]. Here  $T(r)$  refers to the stellar temperature profile as function of radius  $r$ . In this paper we adopt  $v_0 = v_T(m_\chi = 20 \text{ GeV}, r = 0) = 110 \text{ km s}^{-1}$  in the Sun, and provide a simple means for rescaling our results to other values of  $v_0$ . Our chosen value is comparable to the typical relative velocities in direct detection experiments, where  $v_0 \sim 250 \text{ km s}^{-1}$  is often employed. Similarly for  $q_0$ , where our default is  $q_0 = 40 \text{ MeV}$ : this is about the typical momentum transferred both in thermal collisions in the Sun and direct detection. This value corresponds to nuclear recoil energies of  $E_R = q^2/2m_{\text{nuc}} \sim 10 \text{ keV}$  in direct detection experiments. As for  $v_0$ , our results can be easily rescaled to any other  $q_0$ ; the process is described in the passage following (72).

In this paper we will not focus on specific particle physics models or the WIMP-nucleon couplings they give rise to. Rather, we will take the general forms (1) and (2), and compute the effect on thermal conduction by an additional heavy species inside a star.

### III. THERMAL CONDUCTION IN A STAR

#### A. Theory

The theoretical framework of energy transport by WIMPs was constructed in detail by Gould and Raffelt [1]. Transport by a weakly-coupled species can occur in two distinct regimes. If the typical inter-scattering distance  $l_\chi$  of a particle  $\chi$  is much larger than the typical geometric length scale  $r_\chi$  (which in this case is the length scale of the WIMP distribution in a star, not the stellar radius), one reaches the Knudsen limit of non-local transport. In the opposite regime, the Knudsen number  $K \equiv l_\chi/r_\chi$  is  $\ll 1$ , and WIMPs scatter many times per scale height as they travel through the medium. Here we are interested in the latter regime, where local thermal equilibrium (LTE) holds.

In [1], Gould and Raffelt analysed the conduction of energy by a collection of massive particles  $\chi$  in the LTE regime. They modelled energy transport using the Boltzmann collision equation:

$$DF = l_\chi^{-1} CF. \quad (4)$$

$F(\mathbf{u}, \mathbf{r}, t)$  here is the phase space density for particle velocity  $\mathbf{u}$  and position  $\mathbf{r}$  at time  $t$ . The typical inter-scattering distance for a WIMP is the inverse of the mean number of interactions it undergoes per unit length

$$l_\chi(\mathbf{u}, \mathbf{r}) = \left[ \sum_i n_i(\mathbf{r}) \langle \sigma_i(\mathbf{u}) \rangle \right]^{-1}, \quad (5)$$

where the index  $i$  denotes the individual nuclear species present in the stellar gas, and the angular brackets represent thermal averaging. The relative weighting of different WIMP velocities in the thermal average depends on the local WIMP velocity distribution, which is itself a function of the temperature with height in the star  $T(\mathbf{r})$ ; the thermal averaging is therefore itself understood to be dependent on  $\mathbf{r}$ . The differential operator is  $D(\mathbf{u}, \mathbf{r}, t) = \partial_t + \mathbf{u} \cdot \nabla_{\mathbf{r}} + \mathbf{g}(\mathbf{r}) \cdot \nabla_{\mathbf{u}}$ , where  $\mathbf{g}(\mathbf{r})$  is the gravitational acceleration.

To proceed, we make three key approximations:

1. The dilute gas approximation: WIMP-WIMP interactions can be neglected because they are much less frequent than WIMP-nucleon interactions.
2. Local isotropy: this allows us to drop any  $\theta, \phi$  dependence in the collision operator  $C$ .
3. The conduction approximation: energy transport is conductive if  $l_\chi$  is smaller than the other two length scales in the problem. That is,

- $l_\chi \ll r_\chi \implies K \ll 1$ , i.e. local thermal equilibrium.
- $l_\chi \ll |\nabla \ln T(\mathbf{r})|^{-1}$ , i.e. the typical inter-scattering distance is much smaller than

the length scale over which the temperature changes. This means that  $\varepsilon \equiv l(r)|\nabla \ln T(r)| \ll 1$ , allowing a perturbative expansion in powers of  $\varepsilon$ .

Actually the first part of approximation 3 is only strictly necessary for the computation of  $\alpha$  and  $\kappa$  rather than their application, as correction factors exist for making the conduction treatment approximately applicable even in the non-local regime when  $K > 1$  (see e.g. [32, 50]). We will discuss these explicitly in Section V.

The collision operator  $C$  has a straightforward intuitive definition:  $CF$  is a function of the WIMP velocity  $\mathbf{u}$ , position  $\mathbf{r}$  and time  $t$ , and represents the local rate of change of the WIMP phase space distribution. It can be formally written in terms of the components  $C_{\text{in}}$  and  $C_{\text{out}}$ ,

$$CF = \int d^3v C'(\mathbf{u}, \mathbf{v}, \mathbf{r}, t) F(\mathbf{v}, \mathbf{r}, t), \text{ with} \quad (6)$$

$$C' \equiv C_{\text{in}}(\mathbf{u}, \mathbf{v}, \mathbf{r}, t) - C_{\text{out}}(\mathbf{v}, \mathbf{r}, t) \delta^3(\mathbf{v} - \mathbf{u}). \quad (7)$$

$C_{\text{in}}(\mathbf{u}, \mathbf{v}, \mathbf{r}, t)$  is the rate at which particles with velocity  $\mathbf{v}$  are scattered to velocity  $\mathbf{u}$ .  $C_{\text{out}}(\mathbf{v}, \mathbf{r}, t)$  is the rate at which particles with velocity  $\mathbf{v}$  are scattered to any other velocity. Performing the integral of  $C_{\text{in}}$  in (6) over incoming velocities  $\mathbf{v}$  gives the total rate of scattering to velocity  $\mathbf{u}$  from any velocity, whereas the integral over  $C_{\text{out}}$  gives the total rate of scattering from velocity  $\mathbf{u}$  to any other velocity. The difference in these two rates is therefore the net rate of change in the WIMP phase space distribution.

The BCE was solved by [1] perturbatively, with the expansion

$$F = F_0 + \varepsilon F_1 + \dots \quad (8)$$

where  $\varepsilon \ll 1$  is an expansion parameter (as explained above),<sup>3</sup> and  $F_0$  is a regular Boltzmann distribution. Such a distribution is in thermal equilibrium by definition, so  $CF_0 = 0$ . Using this expansion to first order, dropping the term  $\varepsilon DF_1$  because it is much smaller than  $DF_0$ , the first order BCE is

$$DF_0 = \frac{\varepsilon}{l_\chi} CF_1. \quad (9)$$

Assuming that the thermal timescale in a star is sufficiently long compared to the timescale for conductive energy transport by multiple WIMP scatterings, the solution of the BCE will be time-independent (stationary),

<sup>3</sup> Note that in the case where the temperature gradient in a stellar core is so steep that  $\varepsilon$  is not small, the entire treatment of energy transport by WIMPs presented here and in [1] breaks down because a perturbative expansion is not possible, even though  $K$  may still be much less than 1. In such interesting cases the phase-space distribution would be strongly non-Boltzmannian, and an entirely different solution to the BCE would be required.

such that the time-derivative in  $D$  can be ignored. In this case, the left-hand side of (9) is

$$DF_0(\mathbf{u}, r) = \frac{\varepsilon}{l_\chi} \left[ \alpha(r) + \frac{m_\chi u^2}{2T(r)} \frac{\nabla \ln T(r)}{|\nabla \ln T(r)|} \right] \mathbf{u} F_0(\mathbf{u}, r), \quad (10)$$

where  $\alpha$  is a separation constant. Assuming the stellar temperature gradient to be spherically symmetric, both  $DF_0$  and  $F_1$  are pure dipoles. We can therefore express the BCE entirely in terms of monopole ( $j = m = 0$ ) and dipole ( $j = 1, m = 0, \pm 1$ ) components of the various quantities; this is the Rosseland approximation.

It is convenient to transform our working variables to dimensionless quantities. We define the WIMP-to-nucleus mass ratio

$$\mu \equiv m_\chi / m_{\text{nuc}}, \quad (11)$$

and divide velocities by the local temperature-dependent velocity  $v_T$  (3)

$$\mathbf{x} \equiv \mathbf{v} / v_T, \quad (12)$$

$$\mathbf{y} \equiv \mathbf{u} / v_T, \quad (13)$$

$$\mathbf{z} \equiv \mathbf{v}_{\text{nuc}} / v_T, \quad (14)$$

with  $v_{\text{nuc}}$  denoting the velocity of a nucleus.

We also define a dimensionless (angle-dependent, differential) cross-section  $\hat{\sigma}$ , and a total dimensionless (angle-independent, non-differential) cross-section  $\hat{\sigma}_{\text{tot}}$ . The total dimensionless cross-section is simply  $\hat{\sigma}$  integrated over the centre-of-mass scattering angle  $\theta_{\text{CM}}$ :

$$\hat{\sigma}_{\text{tot}}(v_{\text{rel}}) \equiv \int_{-1}^1 d \cos \theta_{\text{CM}} \hat{\sigma}(v_{\text{rel}}, q), \quad (15)$$

remembering that  $q$  is itself a function of both  $v_{\text{rel}}$  and  $\cos \theta_{\text{CM}}$ . The original dimensionless differential cross-section ( $\hat{\sigma}$ ) is defined by the requirement that the total dimensionless cross-section be unity at  $v_{\text{rel}} = v_T$ , i.e.

$$\hat{\sigma}_{\text{tot}}(v_T) = 1. \quad (16)$$

Similarly, we define the normalised phase space distribution functions

$$f_n^{j,m} \equiv \frac{1}{n_{\chi, \text{LTE}}(r)} F_n^{j,m}, \quad (17)$$

where  $n_{\chi, \text{LTE}}(r)$  is the WIMP number density in the LTE (conductive) approximation,  $n$  is the expansion order in  $\varepsilon$ ,  $j$  is the degree and  $m$  is the order of the spherical harmonic expansion.

The first order equation (9) can then be expressed as the combination of

$$(\alpha_m y - \delta_{m0} y^3) f_0^{0,0}(y, r) = \int dx C(y, x, r) f_1^{1,m}(x, r) \quad (18)$$

and the stationarity condition, expressed as the absence of a net WIMP flux across any given surface inside the star:

$$\int dx x f_1^{1,m}(x, r) = 0. \quad (19)$$



Here  $\alpha_m$  are thermal diffusivity coefficients corresponding to the dipole coefficients in the spherical harmonic expansion of  $\hat{\mathbf{u}} \cdot \boldsymbol{\alpha}(r)$ . In the Dirac notation of [1], where

$$|f\rangle \equiv f(y), \quad (20)$$

$$Q|f\rangle \equiv \int dx Q(y, x)f(x), \quad (21)$$

$$\langle g|f\rangle \equiv \int dx g(x)f(x), \quad (22)$$

$$\langle g|Q|f\rangle \equiv \int dy dx g(y)Q(y, x)f(x), \quad (23)$$

we see that (18) and (19) become quite compact:

$$\alpha_m(r)|yf_0^{0,0}\rangle - \delta_{m0}|y^3 f_0^{0,0}\rangle = C|f_1^{1,m}\rangle, \quad (24)$$

$$\langle y|f_1^{1,m}\rangle = 0. \quad (25)$$

In terms of the inverse of the collisional operator  $C$ , we can write the solution to the first-order BCE as

$$|f_1^{1,m}\rangle = \alpha_m C^{-1}|yf_0^{0,0}\rangle - \delta_{m0}C^{-1}|y^3 f_0^{0,0}\rangle. \quad (26)$$

The diffusivity coefficients are then fully specified by multiplying (26) by  $\langle y|$ :

$$\alpha_{\pm 1} = 0, \quad (27)$$

$$\alpha_0 = \frac{\langle y|C^{-1}|y^3 f_0^{0,0}\rangle}{\langle y|C^{-1}|yf_0^{0,0}\rangle}. \quad (28)$$

This can be used to obtain the stationary WIMP density profile [1]

$$n_{\chi, \text{LTE}}(r) = n_{\chi, \text{LTE}}(0) \left[ \frac{T(r)}{T(0)} \right]^{3/2} \times \exp \left[ - \int_0^r dr' \frac{k_B \alpha(r') \frac{dT(r')}{dr'} + m_\chi \frac{d\phi(r')}{dr'}}{k_B T(r')} \right], \quad (29)$$

where  $\phi(r)$  refers to the gravitational potential at height  $r$  in the star. Together with the thermal conductivity  $\kappa$

$$\kappa = \frac{\sqrt{2}}{3} \langle y^3 |f_1^{1,0}\rangle, \quad (30)$$

one can then use (29) to finally obtain the luminosity carried by WIMP scattering,

$$L_{\chi, \text{LTE}}(r) = 4\pi r^2 \zeta^{2n}(r) \kappa(r) n_{\chi, \text{LTE}}(r) l_\chi(r) \times \left[ \frac{k_B T(r)}{m_\chi} \right]^{1/2} k_B \frac{dT(r)}{dr}, \quad (31)$$

and the corresponding energy injection rate per unit mass of stellar material:

$$\epsilon_{\chi, \text{LTE}}(r) = \frac{1}{4\pi r^2 \rho(r)} \frac{dL_{\chi, \text{LTE}}(r)}{dr}. \quad (32)$$

Here  $\rho(r)$  is the stellar density,  $\zeta(r) = v_0/v_T(r)$  for velocity-dependent scattering and  $\zeta(r) = q_0/[m_\chi v_T(r)]$  for momentum-dependent scattering. The factors of  $\zeta$  in

(31) connect the velocity (momentum) scale at which the reference cross-section  $\sigma_0$  is defined, to the thermal scale  $v_T$  ( $m_\chi v_T$ ) at which the dimensionless conductivity  $\kappa$  is computed. Note that as per Ref. [32], our sign convention is such that positive  $L$  and  $\epsilon$  refer to energy injection rather than evacuation, which differs from Ref. [1].

The problem of calculating the rate of energy transport by WIMPs is now one of explicitly calculating  $\alpha$  and  $\kappa$  for the WIMP-nucleus mass ratio and cross-section of interest. Gould and Raffelt [1] did this calculation for a range of mass ratios, but only the case of velocity- and momentum-independent cross-sections; here we extend the treatment to more general cross-sections.

## B. Calculations of $\alpha$ and $\kappa$

Because we plan on evaluating the collision operator  $C$  numerically, it makes sense to express the functions  $|f(y)\rangle$  as one-dimensional ‘‘vectors’’ and the operators as two-dimensional matrices. This allows direct calculation of a well-defined inverse operator  $C^{-1}$ , simply by inverting the corresponding matrix for  $C$ . Although the integrals of the form  $Q|f(y)\rangle$  are from zero to infinity, the exponential behaviour of  $f(y)$  means that the  $y > 3$  contribution to each integral is less than a fraction of a percent. We therefore truncate the vectors and matrices at  $y = 5$ .

$C_{\text{out}}$  is relatively straightforward to construct:

$$C_{\text{out}}(x, r) = \int d^3 z |\mathbf{x} - \mathbf{z}| \hat{\sigma}_{\text{tot}}(v_T |\mathbf{x} - \mathbf{z}|) F_{\text{nuc}}(\mathbf{z}), \quad (33)$$

where  $F_{\text{nuc}}(\mathbf{z})$  is the velocity distribution of the nuclei,

$$F_{\text{nuc}}(\mathbf{z}) = (\pi\mu)^{-3/2} e^{-|\mathbf{z}|^2/\mu}. \quad (34)$$

An expression for  $C_{\text{in}}$  is not as obvious. We transform to centre of mass (CM) coordinates, where  $\mathbf{a}$  is the velocity of the CM frame, and  $\mathbf{b}$  and  $\mathbf{b}'$  are respectively the incoming and outgoing WIMP velocities in that frame.<sup>4</sup> These quantities are illustrated in Figure 1.

Ref. [1] then finds

$$C_{\text{in}}^j(y, x, r) = (1 + \mu)^4 \frac{y}{x} \int_0^\infty da \int_0^\infty db F_{\text{nuc}}(\mathbf{z}) 2\pi b \langle P_j \hat{\sigma} \rangle \times \Theta(y - |a - b|) \Theta(a + b - y) \times \Theta(x - |a - b|) \Theta(a + b - x). \quad (35)$$

$\langle P_j(\cos \theta_{\text{lab}}) \hat{\sigma} \rangle$  is the angle-averaged product of the differential cross-section with the  $j$ -th Legendre polynomial, as expanded around transverse scattering angles in the lab frame. The angle averaging is performed in the azimuthal direction around the  $\mathbf{a}$  axis in the CM frame. The integral over the zenith angle is performed implicitly when

<sup>4</sup> In the language of Ref. [1]  $\mathbf{a}$  and  $\mathbf{b}$  correspond to  $\mathbf{s}$  and  $\mathbf{t}$ , respectively.

TABLE I. Analytic forms of the integral (33), given as a function of  $w \equiv y/\sqrt{\mu}$ . Expressions are identical for velocity-dependent and momentum-dependent cross-sections of the same order  $2n$ .

$\sigma = \text{const.}$	$C_{\text{out}}(y) = \mu^{1/2} \left[ \left( w + \frac{1}{2w} \right) \text{erf}(w) + \frac{1}{\sqrt{\pi}} \exp(-w^2) \right]$
$\sigma \propto v_{\text{rel}}^2, q^2$	$C_{\text{out}}(y) = \mu^{3/2} \left[ \frac{3+12w^2+4w^4}{4w} \text{erf}(w) + \frac{5+2w^2}{2\sqrt{\pi}} \exp(-w^2) \right]$
$\sigma \propto v_{\text{rel}}^4, q^4$	$C_{\text{out}}(y) = \mu^{5/2} \left[ \frac{(15+8w^6+60w^4+90w^2)}{8w} \text{erf}(w) + \frac{(33+4w^4+28w^2)}{4\sqrt{\pi}} \exp(-w^2) \right]$
$\sigma \propto v_{\text{rel}}^{-2}, q^{-2}$	$C_{\text{out}}(y) = \mu^{-1/2} w^{-1} \text{erf}(w)$

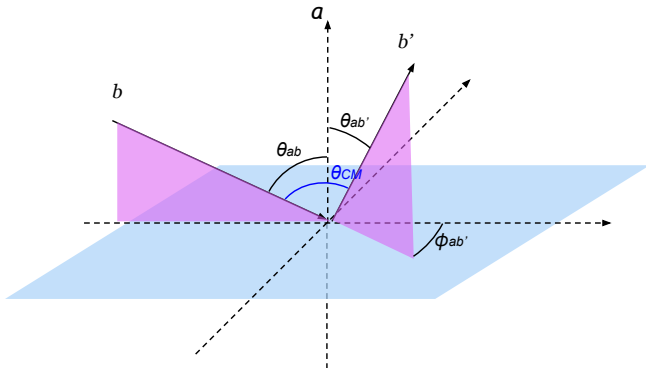


FIG. 1. Scattering kinematics in the centre of mass frame, for the computation of  $C_{\text{in}}$ . The velocity of the CM with respect to the lab frame is  $a$ . The incoming and outgoing WIMP velocities are  $b$  and  $b'$  respectively. Nucleon velocities are not shown, as they are simply related to the WIMP quantities in this frame.

integrating over  $a$  and  $b$ . Note that in this angle-average,  $P_j$  is a function of  $\theta_{\text{lab}}$ , whereas  $\hat{\sigma}$  is a function of  $v_{\text{rel}}$  and  $\theta_{\text{CM}}$ . The two angles are related as

$$\cos \theta_{\text{CM}} = A + B \cos \phi_{ab'}, \quad (36)$$

$$\cos \theta_{\text{lab}} = G + B \frac{b^2}{xy} \cos \phi_{ab'}, \quad (37)$$

$$(38)$$

with

$$A \equiv \cos \theta_{ab'} \cos \theta_{ab} = \frac{(x^2 - a^2 - b^2)(y^2 - a^2 - b^2)}{4a^2b^2}, \quad (39)$$

$$B \equiv \sin \theta_{ab'} \sin \theta_{ab}, \quad (40)$$

$$G \equiv \frac{(x^2 + a^2 - b^2)(y^2 + a^2 - b^2)}{4a^2xy}. \quad (41)$$

As we are only solving the BCE to first order, the only relevant term in (35) is  $\langle P_1 \hat{\sigma} \rangle$ . Noting that  $v_{\text{rel}} = (1 + \mu)bv_T$ , we then have

$$\langle P_j \hat{\sigma} \rangle = \langle P_1 \hat{\sigma} \rangle = \frac{1}{2\pi} \int_0^{2\pi} d\phi_{ab'} \left( G + B \frac{b^2}{xy} \cos \phi_{ab'} \right) \times \hat{\sigma} [(1 + \mu)bv_T, A + B \cos \phi_{ab'}]. \quad (42)$$

#### IV. CONDUCTION COEFFICIENTS FOR NON-STANDARD WIMPS

We write the cross-sections of interest to us explicitly in terms of the dimensionless variables. We will find  $C_{\text{out}}$  will usually have a tractable analytic form, but that the evaluation of the kinematic integrals for  $C_{\text{in}}$  (35) must be done numerically. In every case, we produce an  $N \times N$  linearly-spaced matrix for  $C(y, x)$ , which we explicitly invert to find  $\alpha$ ,  $|f_1^{1,0}(y)|$  and  $\kappa$ . We find  $N = 500$  to be sufficient: both  $\alpha$  and  $\kappa$  vary by less than one part in  $10^5$  when going from  $N = 400$  to  $N = 500$ , across the full range of  $\mu$  values we consider. For the standard  $\sigma = \text{const.}$  case, our method of explicit matrix inversion yields identical results to the values of  $\alpha(\mu)$  and  $\kappa(\mu)$  presented in Table I of Ref. [1], where a slightly different iterative method was used. These values are shown in the figures in this section and are given explicitly in Table II at the end of the text. We have furthermore cross-checked our results for the collision operator  $C_{\text{in}}$  and  $C_{\text{out}}$  as well as the first-order solution  $f_1^{1,0}(y)$  presented in the figures of Ref. [1].

##### A. Velocity-dependent scattering

The relative velocity is the difference between the incoming WIMP speed  $x$  and the nucleus speed  $z$ ; expressed in terms of these velocities, the dimensionless differential cross-section is just

$$\hat{\sigma}_{v^{2n}} = \frac{1}{2} |\mathbf{x} - \mathbf{z}|^{2n}. \quad (43)$$

$C_{\text{out}}$  is then modified by extra powers of the relative velocity. The angular and radial integrals can be performed analytically, and the results are given in Table I.  $C_{\text{in}}$  is also modified in a simple way. The angular dependence drops out in the centre of mass frame where we compute  $C_{\text{in}}$  and  $\mathbf{x} - \mathbf{z} = (1 + \mu)\mathbf{b}$ , so that

$$\hat{\sigma}_{v^{2n}} = \frac{1}{2} (1 + \mu)^{2n} b^{2n}. \quad (44)$$

These are related to (2) via:

$$\sigma = 2\sigma_0 c^{-2n} \hat{\sigma}_{v^{2n}}, \quad (45)$$

where  $\zeta$  is defined below (32). There is one final complication in the computation of  $C_{\text{in}}$  (35) for the  $v^{-2}$  case: the expression (44) diverges for  $b \rightarrow 0$ , complicating the numerical integration of  $C_{\text{in}}$ , even though the integral itself is finite. We address this by imposing a cutoff velocity  $\omega$  such that:

$$\hat{\sigma}_{v^{-2}} \rightarrow \frac{1 + \omega^2}{2(|\mathbf{x} - \mathbf{z}|^2 + \omega^2)} = \frac{1 + \omega^2}{2(1 + \mu)^2 b^2 + 2\omega^2}, \quad (46)$$

where the factor in the numerator ensures that  $\hat{\sigma}_{\text{tot}}(v_T) = 1$ . Both  $\alpha$  and  $\kappa$  converge to finite values as  $\omega^2 \rightarrow 0$ . The thermally-averaged cross-section, necessary for computing a particle's typical inter-scattering distance  $l_\chi$ , can potentially depend on non-zero  $\omega$ . A large value is reasonable, for example, in the case of resonant Sommerfeld-enhanced scattering, where the cross-section can reach a saturation value for  $v_{\text{rel}}/c \approx 10^{-5} - 10^{-3}$ , below which  $\sigma$  becomes constant.

Values of  $C_{\text{in}}(y, x)$  for  $\mu = 1$  are illustrated on the left-hand side of Figure 2. For positive powers of  $v_{\text{rel}}$ , this results in enhanced scattering of particles with high incoming velocity  $v$ ; conversely this enhancement is present a low incoming velocities for  $\sigma \propto v_{\text{rel}}^{-2}$ .

In Figure 3, the thermal conduction coefficients  $\alpha$  and  $\kappa$  are shown for  $v_{\text{rel}}^2$  scattering (blue dashed lines), and for  $v_{\text{rel}}^4$  (cyan dotted lines). For the  $v^{-2}$  case,  $\kappa$  and  $\alpha$  converge to well-defined curve as  $\omega^2 \rightarrow 0$ ; these are the values we show in the bottom panels of Figure 3 (dark red dashed lines), and later use to compute  $L(r)$ . Numerical values are provided in Table II.

The effect of positive powers of  $v_{\text{rel}}$  is to suppress  $\alpha$  at low values of  $\mu$ , and to suppress  $\kappa$  for large values of  $\mu$ .  $\alpha$  is a measure of how well WIMPs can diffuse outward in the potential well of a star. This suppression ultimately means that the distribution  $n_\chi(r)$  will be more compact than in the standard case. The effect of a  $\kappa$  suppression, meanwhile, implies that the WIMP population will be less efficient at heat transport via scattering with light nuclei such as hydrogen. In the lower panel of Figure 3 we show that the opposite behaviour is true for  $\sigma \propto v_{\text{rel}}^{-2}$ : a ‘‘fluffier’’ WIMP distribution around the stellar core, with enhanced heat transport via collisions.

In the case of a large cutoff velocity  $\omega$ , the thermal conduction coefficients lie in between the  $\sigma = \text{const.}$  and  $\sigma \propto v_{\text{rel}}^{-2}$  cases. We illustrate this in Figure 4, for several values of the dimensionless cutoff velocity  $\omega$ . Sommerfeld-enhanced DM models, therefore, would benefit from some of the enhanced conduction of the  $v_{\text{rel}}^{-2}$  case.

## B. Momentum-dependent scattering

The momentum transferred during a collision,  $q = \sqrt{2m_{\text{nuc}}E_{\text{R}}}$  is equal to the total momentum gained or

lost by the WIMP:

$$\begin{aligned} q^2 &= m_\chi^2 |\mathbf{u} - \mathbf{v}|^2 \\ &= q_0^2 \zeta^{-2} |\mathbf{x} - \mathbf{y}|^2 \\ &= 2b^2 \zeta^{-2} q_0^2 (1 - \cos \theta_{\text{CM}}). \end{aligned} \quad (47)$$

The latter expression allows us to write the cross-section in terms of the centre-of-mass velocity of the incoming WIMP,  $b$ , and the CM scattering angle  $\theta_{\text{CM}}$ , as the scattering event does not change the WIMP's speed in the CM frame, only its direction.

Then

$$\hat{\sigma}_{q^{2n}} = 2^{-n} H_n |\mathbf{x} - \mathbf{y}|^{2n} = H_n b^{2n} (1 - \cos \theta_{\text{CM}})^n, \quad (48)$$

where the normalisation factor required to ensure that  $\hat{\sigma}_{\text{tot}}(v_T) = 1$  is

$$H_n = \frac{(1 + \mu)^{2n}}{\int_{-1}^1 (1 - \cos \theta')^n d \cos \theta'}. \quad (49)$$

The structure of (48) shows us that

$$\hat{\sigma}_{q^{2n}} = 2\hat{\sigma}_{v^{2n}} \frac{(1 - \cos \theta_{\text{CM}})^n}{\int_{-1}^1 (1 - \cos \theta')^n d \cos \theta'}, \quad (50)$$

so

$$\hat{\sigma}_{\text{tot}, q^{2n}} = \hat{\sigma}_{\text{tot}, v^{2n}} = (1 + \mu)^{2n} b^{2n}, \quad (51)$$

as we would expect, given that  $\hat{\sigma}_{\text{tot}}$  is independent of  $\theta_{\text{CM}}$ . This also means that  $C_{\text{out}, q^{2n}} = C_{\text{out}, v^{2n}}$ . In terms of the dimensionful cross-section (1),

$$\sigma = \frac{2^n}{H_n} \sigma_0 \zeta^{-2n} \hat{\sigma}_{q^{2n}}. \quad (52)$$

The component  $C_{\text{in}}$  requires an explicit evaluation of  $\langle P_1 \hat{\sigma}(\cos \theta_{\text{CM}}) \rangle$ :

$$\langle P_1 \hat{\sigma}_0 \rangle = \frac{1}{2} G, \quad (53)$$

$$\langle P_1 \hat{\sigma}_{q^2} \rangle = \frac{1}{2} b^2 (1 + \mu)^2 \left[ G(1 - A) - \frac{b^2 B^2}{2xy} \right], \quad (54)$$

$$\begin{aligned} \langle P_1 \hat{\sigma}_{q^4} \rangle &= \frac{3}{8} b^4 (1 + \mu)^4 \left[ \left\{ G(1 - A) - \frac{b^2 B^2}{xy} \right\} (1 - A) \right. \\ &\quad \left. + \frac{GB^2}{2} \right], \end{aligned} \quad (55)$$

$$\begin{aligned} \langle P_1 \hat{\sigma}_{q^{-2}} \rangle &= \frac{1}{\ln 2 - \ln \xi} b^{-2} (1 + \mu)^{-2} \\ &\quad \times \left[ \frac{(1 - A + \xi)b^2 + Gxy}{xy \sqrt{(1 - A + \xi)^2 - B^2}} - \frac{b^2}{xy} \right], \end{aligned} \quad (56)$$

where  $A$ ,  $B$  and  $G$  are defined in (39–41). The parameter  $\xi$  comes from the replacement  $\cos \theta_{\text{CM}} \rightarrow \cos \theta_{\text{CM}} - \xi$ . We make this substitution because for  $n = -1$ , the factor  $(1 - \cos \theta)^{-1}$  in (48) causes the cross-section to diverge for

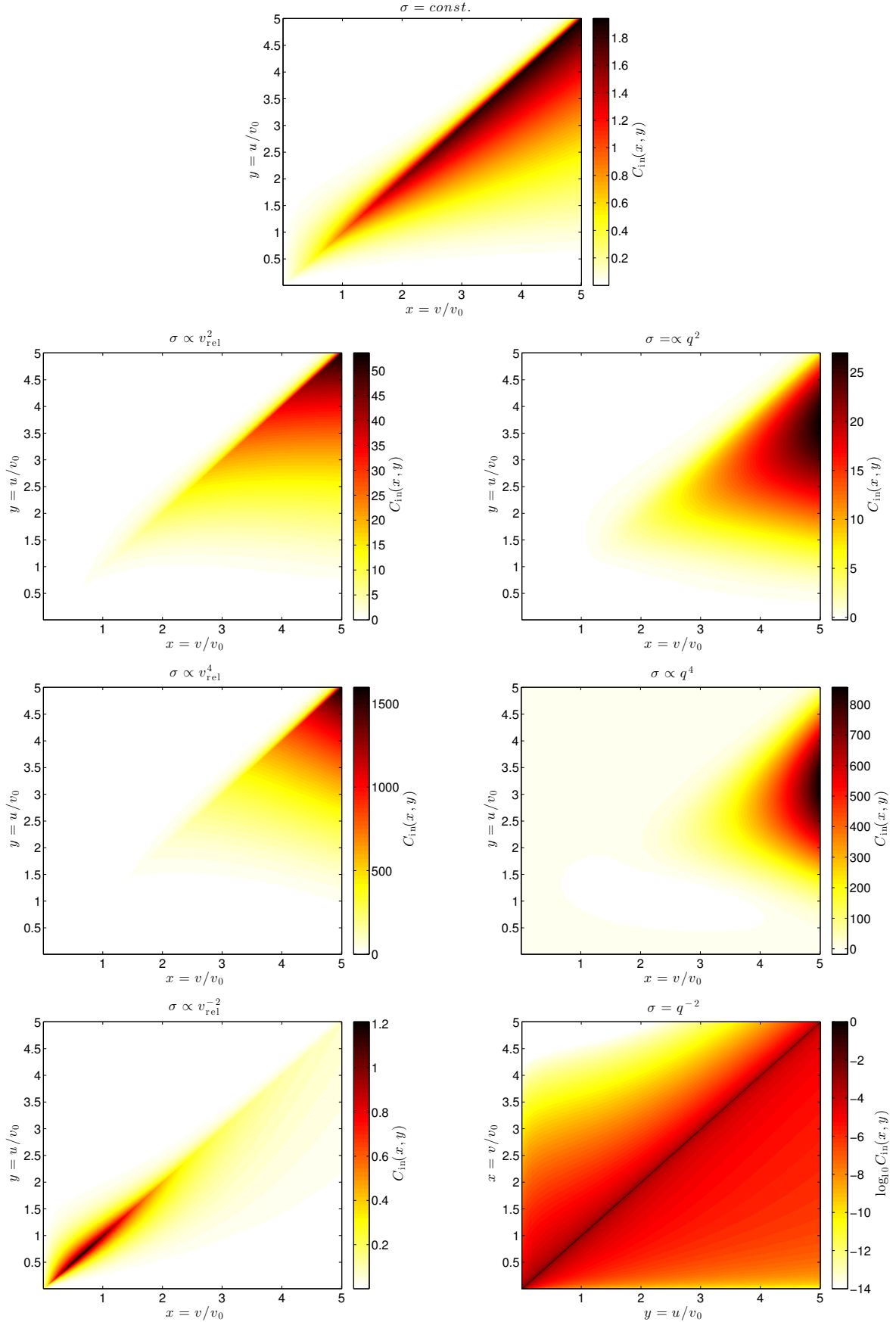


FIG. 2. Partial dimensionless collision operator  $C_{\text{in}}(y, x)$  with  $\mu = m_\chi/m_{\text{nuc}} = 1$  for the various types of cross-section, as a function of the WIMP's dimensionless incoming velocity  $x$  and outgoing velocity  $y$ . The angular integral in the  $q^{-2}$  case (bottom-right panel) is regulated with  $\xi = 10^{-8}$  (56) to remove the divergence at  $x = y$ . Note also the log scale in this panel.



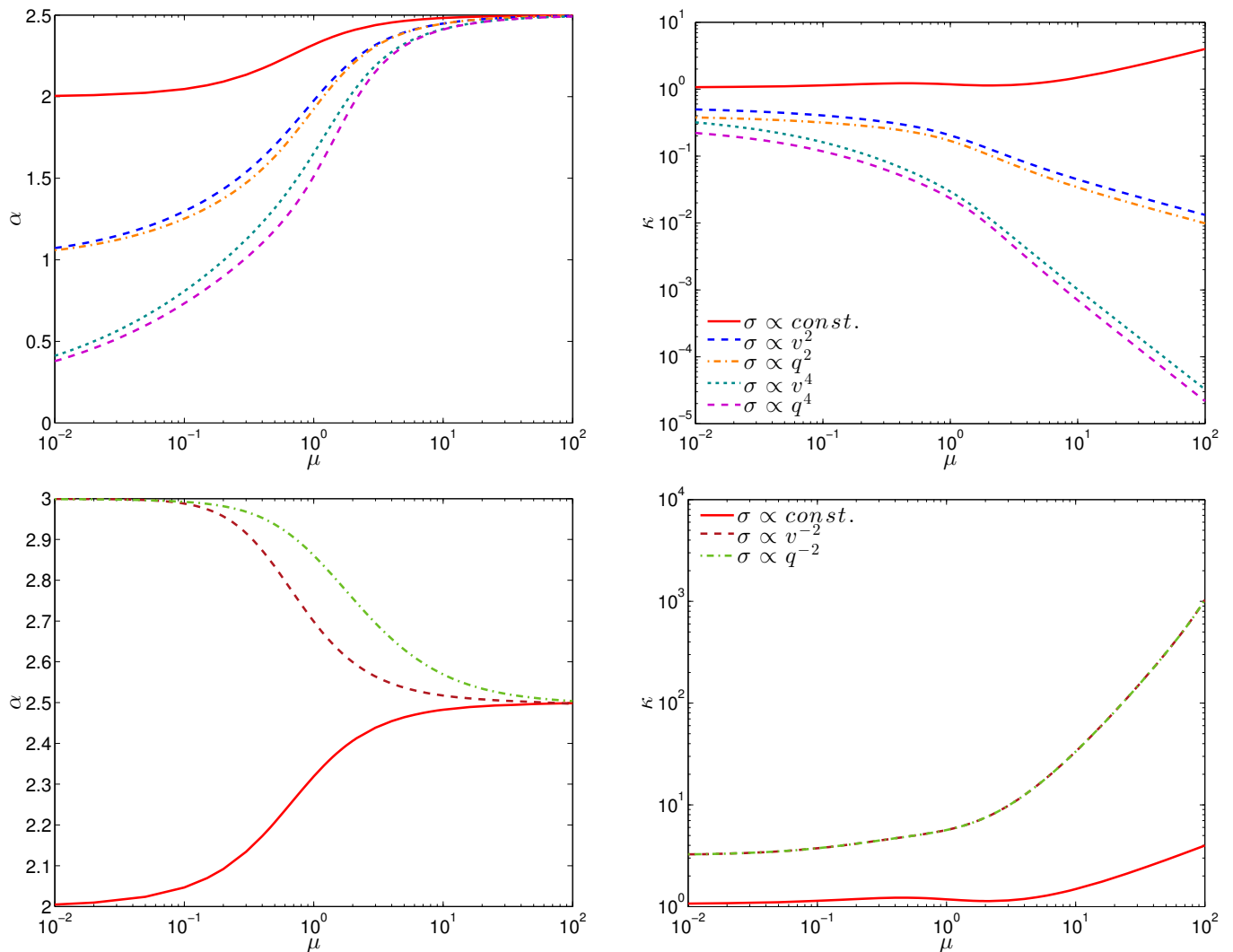


FIG. 3. Dimensionless thermal diffusivity  $\alpha$  (left) and conductivity  $\kappa$  (right) as a function of  $\mu = m_\chi/m_{\text{nuc}}$ . Curves are shown for velocity-dependent scattering cross-sections  $\sigma \propto v_{\text{rel}}^{2n}$  and for momentum-dependent cross-sections  $\sigma \propto q^{2n}$ . The upper panels show curves for positive values of  $n$ , and bottom panels show results for  $n = -1$ . In every case the thick red line is the fiducial case  $\sigma = \text{const.}$ , which was calculated explicitly by Gould and Raffelt [1]. Note that, because we regulate the cross-section for  $q^{-2}$ -dependent scattering using the momentum transfer cross-section (57), the  $\kappa$  curves for  $v_{\text{rel}}^{-2}$  and  $q^{-2}$  are identical.

forward scattering at small angles; likewise for the integral (15). For the computation of  $\alpha$  in (28), the powers of  $C^{-1}$  allow the divergence to cancel. However,  $\kappa$ , which governs momentum transfer, formally diverges. Fortunately, the divergence at  $\theta_{\text{CM}} = 0$  corresponds to forward scattering, in which no momentum is actually transferred. We regulate this divergence with the ‘‘momentum transfer cross-section,’’ which comes from plasma physics [111] but has also been applied to parameterise transport by WIMPs [112]:

$$\hat{\sigma}_{\text{tot,T}}(v_{\text{rel}}) \equiv \int_{-1}^1 d \cos \theta_{\text{CM}} \hat{\sigma}_{\text{T}}(v_{\text{rel}}, q), \quad (57)$$

$$\hat{\sigma}_{\text{T}}(v_{\text{rel}}, q) \equiv (1 - \cos \theta_{\text{CM}}) \hat{\sigma}(v_{\text{rel}}, q), \quad (58)$$

where  $\hat{\sigma}$  is as per (48), but with the replacement  $n \rightarrow n+1$

in the denominator of (49). This gives

$$\langle P_1 \hat{\sigma}_{\text{T},q^{-2}} \rangle = \frac{1}{2} \frac{G}{b^2(1+\mu)^2}, \quad (59)$$

leading to a finite, well-defined value of  $\kappa$ .

The behaviour of  $C_{\text{in}}$  as a function of  $x$  and  $y$  for momentum-dependent cross-sections is shown in the right-hand panels of figure 2. The two upper right-hand panels show an enhancement in the scattering rate when the momentum transfer is large, over both the constant and velocity-dependent cases, which favour collisions closer to the  $x = y$  line. The lower-right panel shows the  $q^{-2}$  case computed with (56) and  $\xi = 10^{-8}$ , illustrating the divergent behaviour in the forward-scattering rate, and a general suppression of collisions which lead to appreciable momentum exchange.

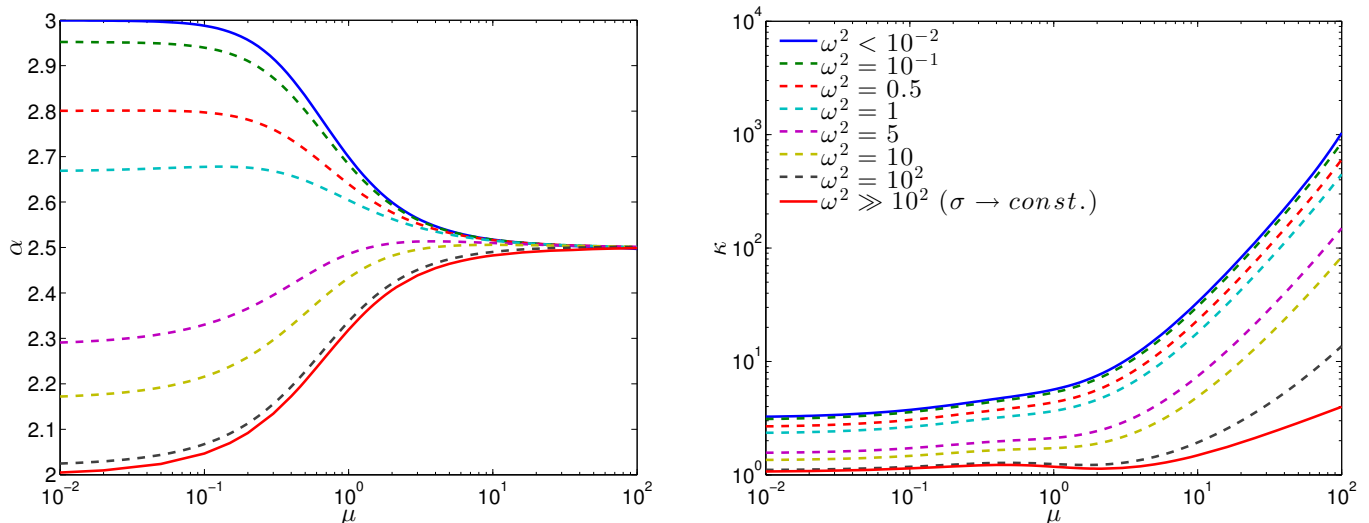


FIG. 4. The effect of a cutoff  $\omega$  to the enhancement on  $\alpha$  and  $\kappa$ , as defined in (46). Increasing the cutoff from  $\omega = 0$  to  $\omega \gg 1$  smoothly transforms  $\alpha$  and  $\kappa$  from the  $\sigma \propto v_{\text{rel}}^{-2}$  case to the  $\sigma = \text{const.}$  case. This type of behaviour could occur, for example, in models of Sommerfeld-enhanced DM scattering, which corresponds to an attractive force with a massive force carrier.

The values of  $\alpha$  and  $\kappa$  are shown in dot-dashed orange for the  $q^2$  case and in dot-dashed green for  $q^{-2}$  in Figure 3. The  $q^4$  case is also shown (dashed purple lines). The behaviour of  $\alpha$  and  $\kappa$  for a  $q^{2n}$  cross-section is qualitatively similar to the  $v_{\text{rel}}^{2n}$  case. Indeed,  $\kappa$  is identical for the  $q^{-2}$  and  $v^{-2}$  cases, thanks to the momentum-transfer cross-section, which essentially deletes the angular dependence in the  $q^{-2}$  case and makes  $C$  identical for momentum and velocity-dependent cross-sections when  $n = -1$ . In the next section we will show that, once this behaviour is combined with the different typical inter-scattering distances in models with momentum-dependent and velocity-dependent scattering, the conduction of energy can be greatly modified with respect to the fiducial constant cross-section case.

## V. EFFECT ON ENERGY TRANSPORT IN THE SUN

We now illustrate the effect of a non-standard WIMP-nucleon cross-section on the conduction of energy within the Sun. Our discussion applies equally well to any star, but modelling and measurements of the Sun and its properties are far more precise than for other stars. We use the temperature, density and elemental composition profiles of the AGSS09ph solar model<sup>5</sup> [65, 71].

Scattering cross-sections  $\sigma_0 \lesssim 10^{-38} \text{ cm}^2$  allowed by bounds from direct detection experiments can easily lead to energy transport outside the LTE regime, i.e. non-local transport. To account for this, based on the results

of Gould & Raffelt [1, 113], Refs. [32, 50] introduce the quantities:

$$\mathfrak{h}(r) = \left( \frac{r - r_\chi}{r_\chi} \right)^3 + 1, \quad (60)$$

$$\mathfrak{f}(K) = \frac{1}{1 + \left( \frac{K}{K_0} \right)^{1/\tau}}, \quad (61)$$

where  $K$  is the Knudsen number,  $K_0 \simeq 0.4$  and  $\tau \simeq 0.5$ . The WIMP scale height  $r_\chi$  as a function of the central temperature  $T_c$  and density  $\rho_c$  is

$$r_\chi = \left( \frac{3k_B T_c}{2\pi G \rho_c m_\chi} \right)^{1/2}. \quad (62)$$

The WIMP distribution becomes a combination of the isothermal and LTE distributions:

$$n_\chi(r) = \mathfrak{f}(K)n_{\chi,\text{LTE}} + [1 - \mathfrak{f}(K)]n_{\chi,\text{iso}}, \quad (63)$$

where

$$n_{\chi,\text{iso}}(r, t) = N(t) \frac{e^{-\frac{r^2}{r_\chi^2}}}{\pi^{3/2} r_\chi^3}. \quad (64)$$

The total luminosity can be finally written:

$$L_{\chi,\text{total}}(r, t) = \mathfrak{f}(K)\mathfrak{h}(r, t)L_{\chi,\text{LTE}}(r, t). \quad (65)$$

For the calculation of WIMP conductive luminosities, we require the typical inter-scattering distance (5), which depends on the local velocity-averaged scattering cross-section. Taking a Maxwell-Boltzmann distribution for the velocities of the WIMPs and nuclei once more, the

<sup>5</sup> publicly available at <http://www.mpa-garching.mpg.de/~aldos/>

distribution of their relative velocities, in normalised units, is

$$F_{\chi-n}(\mathbf{x} - \mathbf{z}) = [\pi(1 + \mu)]^{-3/2} e^{-\frac{|\mathbf{x}-\mathbf{z}|^2}{1+\mu}}. \quad (66)$$

This then gives:

$$\langle \sigma_{v^2} \rangle = \sigma_0 \zeta^{-2} \left\langle \frac{v_{\text{rel}}^2}{v_T^2} \right\rangle = \frac{3}{2} \sigma_0 \zeta^{-2} (1 + \mu), \quad (67)$$

$$\langle \sigma_{v^4} \rangle = \sigma_0 \zeta^{-4} \left\langle \frac{v_{\text{rel}}^4}{v_T^4} \right\rangle = \frac{15}{4} \sigma_0 \zeta^{-4} (1 + \mu)^2, \quad (68)$$

$$\langle \sigma_{v^{-2}} \rangle = \sigma_0 \zeta^2 \left\langle \frac{v_{\text{rel}}^{-2}}{v_T^{-2}} \right\rangle = 2 \sigma_0 \zeta^2 (1 + \mu)^{-1}, \quad (69)$$

where  $\zeta \equiv v_0/v_T$ . The averaged  $q$ -dependent cross-sections follow from these, as  $\langle b^{2n} \rangle = \langle (v_{\text{rel}}/v_0)^{2n} \rangle / (1 + \mu)^{2n}$ :

$$\langle \sigma_{q^2} \rangle = 6 \sigma_0 \zeta^{-2} (1 + \mu)^{-1}, \quad (70)$$

$$\langle \sigma_{q^4} \rangle = 40 \sigma_0 \zeta^{-4} (1 + \mu)^{-2}, \quad (71)$$

$$\langle \sigma_{q^{-2}} \rangle = \sigma_0 \zeta^2 (1 + \mu), \quad (72)$$

where for  $q$ -dependent cross-sections  $\zeta \equiv q_0/m_\chi v_T$ . We have again regulated the divergence in the  $q^{-2}$  case using the momentum transfer cross-section.

Here we take the opportunity to point out that our results for  $\alpha$  and  $\kappa$  are fully independent of  $\zeta$ , and therefore  $v_0$  and  $q_0$ . To apply them in cases where  $v_0$  or  $q_0$  differ from the canonical values we have assumed in this paper, one need only use the desired  $v_0$  or  $q_0$  when implementing (31) and the appropriate one of (67)–(72).

To properly compute the effect of WIMPs in the Sun, we will need to include the conduction coefficients in a full solar evolution code that also includes a detailed computation of the velocity/momentum-dependent capture, evaporation and annihilation rates (if any); that work will appear soon [114]. For the purpose of this paper, we simply assume a steady state with a set number of WIMPs per baryon in the present Sun ( $n_\chi/n_b$ ), in order to directly compare the conductive efficiencies of cross-sections with different velocity and momentum scalings. Likewise, we simply choose a few benchmark values of  $m_\chi$ ,  $\sigma_0$ ,  $v_0$  and  $q_0$  at which to make these comparisons, and assume for the sake of example that  $\sigma_0$  scales with nuclear mass as it does for isospin-conserving spin-independent couplings (i.e. proportional to the square of the atomic number).

In Figure 5 we illustrate the effect on energy transport by 1 GeV and 20 GeV WIMPs in the Sun, using  $n_\chi/n_b = 10^{-16}$  WIMPs per baryon,  $v_0 = 110$  km/s, and  $\sigma_0 = 10^{-39}$  cm<sup>2</sup>. These roughly correspond to results of [52], which provide some small effects on solar structure. The combined effect of  $\alpha$ ,  $\kappa$  and  $l_\chi$  gives a suppression of energy transport in the case of a  $v_{\text{rel}}^2$  or  $v_{\text{rel}}^4$  cross-section, but an enhancement for the  $v_{\text{rel}}^{-2}$  case, due to the increased scattering at low velocity.

Figure 6 shows the absolute energy transported by WIMPs with a momentum-dependent cross-section for  $m_\chi = 1$  GeV and  $m_\chi = 20$  GeV, again with  $n_\chi/n_b =$

$10^{-16}$  WIMPs per baryon and  $\sigma_0 = 10^{-39}$  cm<sup>2</sup>. Here we use  $q_0 = 40$  MeV, which corresponds to a nuclear recoil energy of  $E_R = 11$  keV in a germanium direct detection experiment, and 29 keV in a silicon detector. It is apparent that at higher masses, a  $q^{2n}$  cross-section with negative  $n$  can result in heat transport that is enhanced by many orders of magnitude relative to standard WIMPs with a constant cross-section. At lower masses, the opposite is true: negative  $n$  suppresses heat transport, whereas positive  $n$  can greatly enhance it.

Figure 7 illustrates this point in more detail. Here we show the full dependence of the total transported energy on the WIMP mass  $m_\chi$ , for each type of  $q$ -dependent scaling. We also compare this behaviour for two different example values of  $q_0$ . For  $q_0 = 1$  MeV – corresponding to recoil energies in detectors of only a few eV – the behaviour of  $\epsilon$  as a function of the sign of  $n$  is reversed below  $m_\chi \sim 2$  GeV. The value of  $q_0 = 40$  MeV that we choose for the right-hand figure is closer to the region probed by underground direct detection experiments, and shows a reversal at slightly higher masses, around  $m_\chi \sim 4$  GeV. This shows that for the mass region probed by such experiments, the effects of Solar heat transport can be much larger than previously computed in the  $\sigma = \text{const.}$  case and that for such models, the comparison between experiments and solar effects should be made on a case-by-case basis.

In contrast with the behaviour shown in Figure 7 for  $q$ -dependent scattering, the total energy transported by  $v_{\text{rel}}$ -dependent scattering does not show a reversal with respect to  $n$  when the WIMP mass is changed. This can also be seen by comparing Figures 5 and 6: for  $q$ , the impact depends on WIMP mass, whereas for  $v_{\text{rel}}$ -dependent scattering, negative  $n$  enhances energy transport and positive  $n$  decreases it, independent of the mass. The qualitative difference between the impacts of the WIMP mass for  $v_{\text{rel}}$  and  $q$ -dependent cross-sections is due to the additional factor of  $(1 + \mu)^2$  in the thermally-averaged cross-section for  $q$ -dependent scattering. This adds an additional dependence on WIMP mass to the typical inter-scattering distance, Knudsen number, and therefore the total  $K$ -dependent luminosity suppression.

Again, we stress that to compute an accurate profile of energy transport, one should include the feedback on solar structure itself during stellar evolution.

## VI. DISCUSSION AND CONCLUSION

Figures 5–7 contrast the potential impacts on energy transport in the Sun of nuclear scattering cross-sections with different momentum and velocity scalings. The differences we see suggest that Solar physics will be a very useful complement to direct detection experiments in ruling out or confirming specific forms of  $\sigma(v_{\text{rel}}, q)$ .

It is worth noting that the cross-sections which give rise to enhanced energy transport will also enhance or suppress the capture of DM by the Sun in the first place.

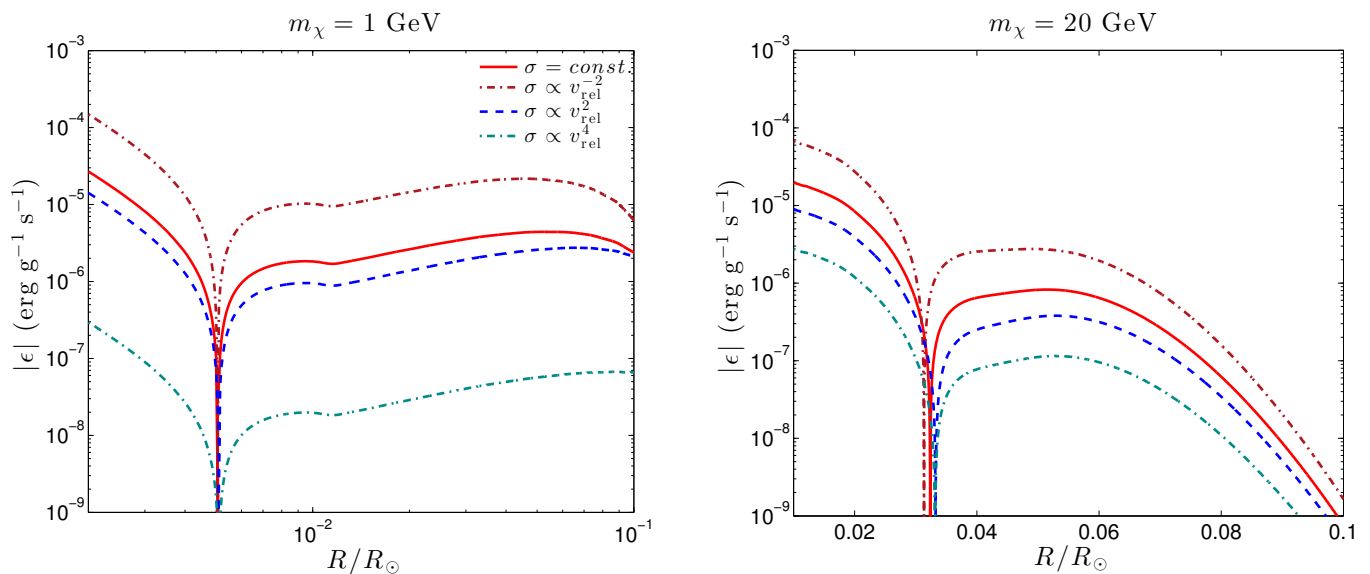


FIG. 5. Absolute energy transported  $|\epsilon|$  by WIMPs of mass  $m_\chi = 1$  GeV (left) and  $m_\chi = 20$  GeV (right) with a velocity dependent cross-section. Transported energy is negative at small  $R$  (below the dip) and becomes positive at larger  $R$ , representing transport from the solar core into outer layers. We have taken the AGSS09ph solar model [71] with  $n_\chi/n_b = 10^{-16}$  WIMPs per baryon,  $v_0 = 110$  km/s, and  $\sigma_0 = 10^{-39}$  cm<sup>2</sup>.

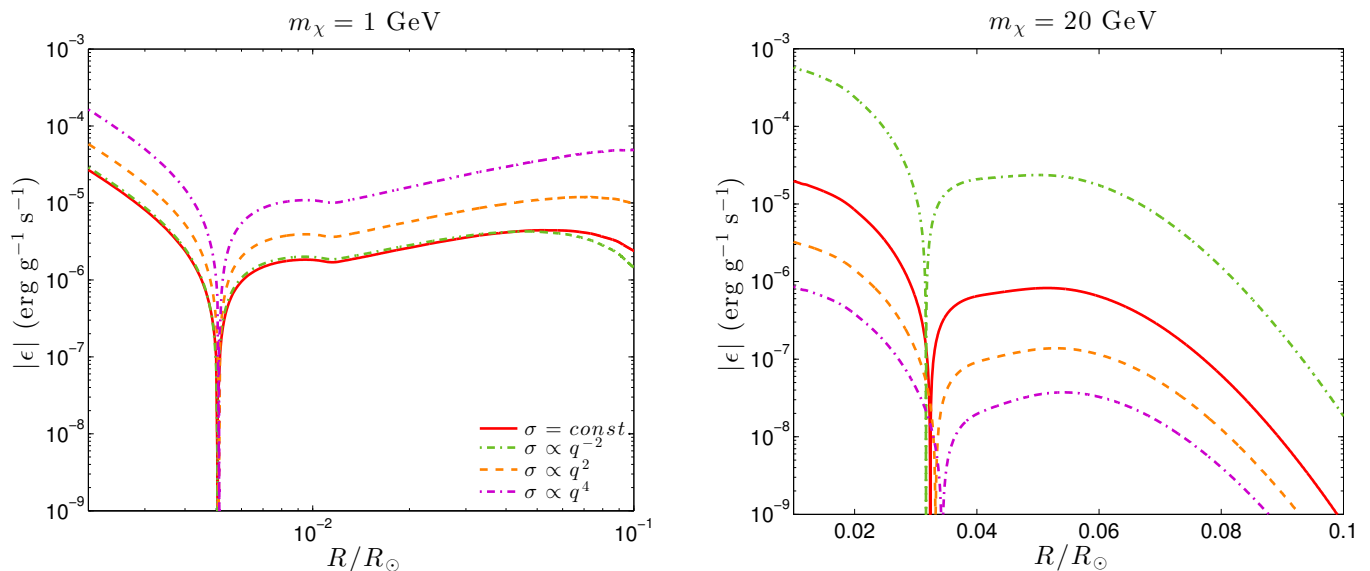


FIG. 6. Absolute energy transported  $|\epsilon|$  by WIMPs of mass  $m_\chi = 1$  GeV (left) and  $m_\chi = 20$  GeV (right) with a momentum-dependent cross-section and  $q_0 = 40$  MeV. We have taken the AGSS09ph solar model [71] with  $n_\chi/n_b = 10^{-16}$  WIMPs per baryon, and  $\sigma_0 = 10^{-39}$  cm<sup>2</sup>.

In order to become gravitationally bound to the Sun, a free WIMP must lose enough kinetic energy to fall below the local escape velocity. A scattering cross-section that goes as  $v^{-2}$  would boost the chance of a free WIMP at the low end of the Galactic DM velocity distribution scattering off a nucleus, whereas a  $q^{2n}$  cross-section with  $n > 0$  would enhance the rate of collisions leading to large enough energy losses for the WIMP's speed to fall below  $v_{\text{esc}}$ . The combination of enhanced capture and

heat transport is therefore expected to lead to observable effects on the solar structure for some models, even for very small scattering cross-sections.

Finally we point out the possible application of this enhanced heat transport to the so-called Solar Abundance Problem. It has been suggested [51, 52] that at intermediate radii,  $m_\chi = 5$  GeV DM can partly reconcile the discrepancy between the results of solar models computed with the latest abundances, and the sound

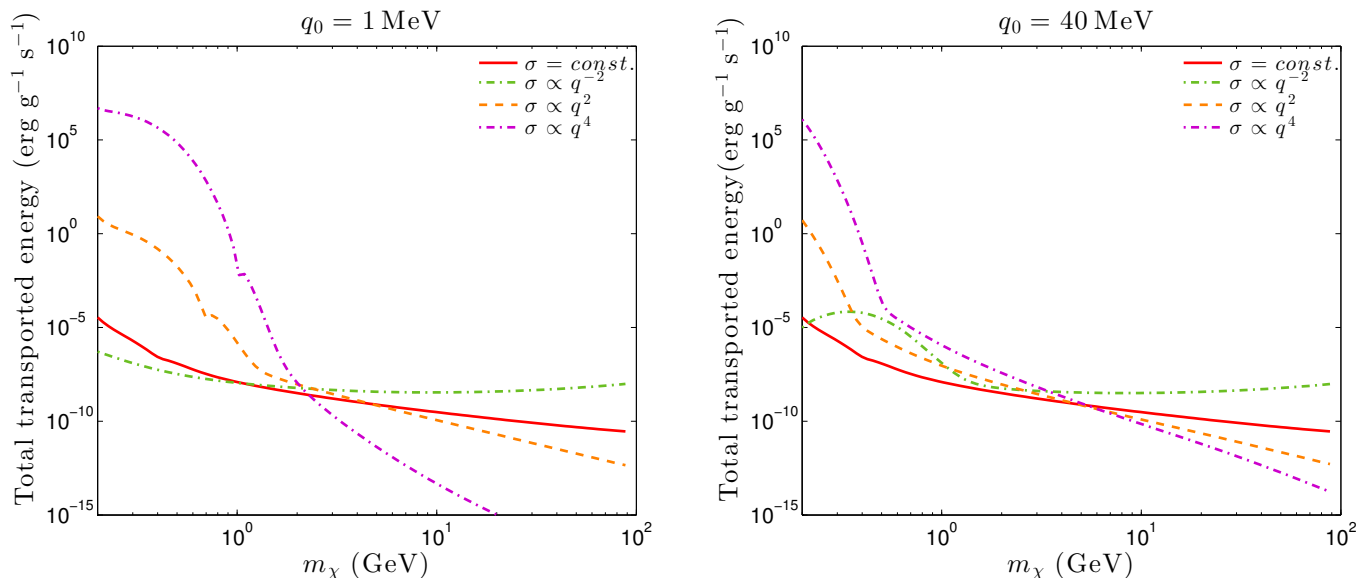


FIG. 7. Total transferred energy  $r_{\odot}^{-3} \int_0^{r_{\odot}} |\epsilon(r)| r^2 dr$  as a function of the WIMP mass for momentum-dependent scattering. Here  $\sigma_0 = 10^{-39} \text{ cm}^2$ ,  $n_{\chi}/n_b = 10^{-16}$  WIMPs per baryon and  $q_0 = 1 \text{ MeV}$  (left) or  $q_0 = 40 \text{ MeV}$  (right). These reference momenta can be compared with nuclear recoil energies in direct detection experiments using the expression  $q_0 = \sqrt{2m_{\text{nuc}}E_R}$ . For recoils on Germanium, for instance, they correspond to nuclear recoil energies of 7 eV and 11 keV, respectively. These show that, depending on the  $q$  region probed by direct detection experiments, solar observations may be far more, or far less sensitive than underground detectors.

speed profile inferred from helioseismology. In this scenario, DM accumulation is usually maximised by taking it to be asymmetric (non-annihilating). However, simulations [53] indicate that the scattering cross-section must be extremely high ( $\sim 10^{-35} \text{ cm}^2$ ) in order to accumulate sufficient quantities of DM to have an observable effect. The enhancement provided to capture and conduction by  $v_{\text{rel}}^{2n}$  or  $q^{2n}$  scattering of DM on nuclei has the potential to finally make DM a viable solution to the abundance problem. There is thus a strong possibility that models such as Sommerfeld-enhanced or dipole DM, whose motivation stem from different areas of DM phenomenology, are particularly suited to resolving this outstanding problem in solar physics.

The framework developed above – an extension of the process established by Gould and Raffelt [1] – allows the computation of the thermal conduction parameters  $\alpha$  and  $\kappa$  for DM particles whose interactions with nuclei are velocity or momentum-dependent. We have computed these parameters explicitly for  $\sigma \propto v_{\text{rel}}^{2n}$  and  $q^{2n}$ , for  $n = \{-1, 1, 2\}$ . Finally, we have shown the impact on heat transfer in the Sun with respect to the fiducial constant  $\sigma$  case, for parameters currently allowed by direct detection experiments. Our results indicate that this impact could be rather substantial. In a follow-up paper we plan to incorporate these results into state-of-the-art Solar simulation software to include realistic DM capture and the feedback on Solar structure itself.

## ACKNOWLEDGEMENTS

AV acknowledges support from FQRNT and European contracts FP7-PEOPLE-2011-ITN and PITN-GA-2011-289442-INVISIBLES. PS is supported by a Banting Fellowship, administered by the Natural Science and Engineering Research Council of Canada.



- [1] A. Gould and G. Raffelt, *Thermal conduction by massive particles*, *ApJ* **352** (1990) 654–668.
- [2] W. H. Press and D. N. Spergel, *Capture by the sun of a galactic population of weakly interacting, massive particles*, *ApJ* **296** (1985) 679–684.
- [3] K. Griest and D. Seckel, *Cosmic asymmetry, neutrinos and the Sun.*, *Nucl. Phys. B* **283** (1987) 681–705.
- [4] A. Gould, *Resonant enhancements in weakly interacting massive particle capture by the earth*, *ApJ* **321** (1987) 571–585.
- [5] G. Steigman, H. Quintana, C. L. Sarazin, and J. Faulkner, *Dynamical interactions and astrophysical effects of stable heavy neutrinos*, *AJ* **83** (1978) 1050–1061.
- [6] D. N. Spergel and W. H. Press, *Effect of hypothetical, weakly interacting, massive particles on energy transport in the solar interior*, *ApJ* **294** (1985) 663–673.
- [7] J. Faulkner and R. L. Gilliland, *Weakly interacting, massive particles and the solar neutrino flux*, *ApJ* **299** (1985) 994–1000.
- [8] L. M. Krauss, M. Srednicki, and F. Wilczek, *Solar System constraints and signatures for dark-matter candidates*, *Phys. Rev. D* **33** (1986) 2079–2083.
- [9] T. K. Gaisser, G. Steigman, and S. Tilav, *Limits on cold-dark-matter candidates from deep underground detectors*, *Phys. Rev. D* **34** (1986) 2206–2222.
- [10] R. Gandhi, J. L. Lopez, D. V. Nanopoulos, K.-j. Yuan, and A. Zichichi, *Scrutinizing supergravity models through neutrino telescopes*, *Phys.Rev.* **D49** (1994) 3691–3703, [[astro-ph/9309048](#)].
- [11] A. Bottino, N. Fornengo, G. Mignola, and L. Moscoso, *Signals of neutralino dark matter from earth and sun*, *Astropart.Phys.* **3** (1995) 65–76, [[hep-ph/9408391](#)].
- [12] L. Bergström, J. Edsjö, and P. Gondolo, *Indirect detection of dark matter in km-size neutrino telescopes*, *Phys. Rev. D* **58** (1998) 103519, [[hep-ph/9806293](#)].
- [13] V. Barger, F. Halzen, D. Hooper, and C. Kao, *Indirect search for neutralino dark matter with high energy neutrinos*, *Phys. Rev. D* **65** (2002) 075022, [[hep-ph/0105182](#)].
- [14] Super-Kamiokande Collaboration: S. Desai, Y. Ashie, *et. al.*, *Search for dark matter WIMPs using upward through-going muons in Super-Kamiokande*, *Phys. Rev. D* **70** (2004) 083523, [[hep-ex/0404025](#)].
- [15] Super-Kamiokande Collaboration: S. Desai, K. Abe, *et. al.*, *Study of TeV neutrinos with upward showering muons in Super-Kamiokande*, *Astropart. Phys.* **29** (2008) 42–54, [[arXiv:0711.0053](#)].
- [16] IceCube Collaboration: R. Abbasi, Y. Abdou, *et. al.*, *Limits on a Muon Flux from Neutralino Annihilations in the Sun with the IceCube 22-String Detector*, *Phys. Rev. Lett.* **102** (2009) 201302, [[arXiv:0902.2460](#)].
- [17] IceCube Collaboration: R. Abbasi, Y. Abdou, *et. al.*, *Limits on a muon flux from Kaluza-Klein dark matter annihilations in the Sun from the IceCube 22-string detector*, *Phys. Rev. D* **81** (2010) 057101, [[arXiv:0910.4480](#)].
- [18] IceCube Collaboration: R. Abbasi, Y. Abdou, *et. al.*, *Multiyear search for dark matter annihilations in the Sun with the AMANDA-II and IceCube detectors*, *Phys. Rev. D* **85** (2012) 042002, [[arXiv:1112.1840](#)].
- [19] Super-Kamiokande Collaboration: T. Tanaka, K. Abe, *et. al.*, *An Indirect Search for Weakly Interacting Massive Particles in the Sun Using 3109.6 Days of Upward-going Muons in Super-Kamiokande*, *ApJ* **742** (2011) 78, [[arXiv:1108.3384](#)].
- [20] P. Scott, C. Savage, J. Edsjö, and the IceCube Collaboration: R. Abbasi *et al.*, *Use of event-level neutrino telescope data in global fits for theories of new physics*, *JCAP* **11** (2012) 57, [[arXiv:1207.0810](#)].
- [21] H. Silverwood, P. Scott, *et. al.*, *Sensitivity of IceCube-DeepCore to neutralino dark matter in the MSSM-25*, *JCAP* **3** (2013) 27, [[arXiv:1210.0844](#)].
- [22] IceCube Collaboration: M. G. Aartsen, R. Abbasi, *et. al.*, *Search for Dark Matter Annihilations in the Sun with the 79-String IceCube Detector*, *Phys. Rev. Lett.* **110** (2013) 131302, [[arXiv:1212.4097](#)].
- [23] P. Salati and J. Silk, *A stellar probe of dark matter annihilation in galactic nuclei*, *ApJ* **338** (1989) 24–31.
- [24] A. Bouquet and P. Salati, *Life and death of cosmions in stars*, *A&A* **217** (1989) 270–282.
- [25] I. V. Moskalenko and L. L. Wai, *Dark Matter Burners*, *ApJ* **659** (2007) L29–L32, [[astro-ph/0702654](#)].
- [26] D. Spolyar, K. Freese, and P. Gondolo, *Dark Matter and the First Stars: A New Phase of Stellar Evolution*, *Phys. Rev. Lett.* **100** (2008) 051101, [[arXiv:0705.0521](#)].
- [27] G. Bertone and M. Fairbairn, *Compact stars as dark matter probes*, *Phys. Rev. D* **77** (2008) 043515, [[arXiv:0709.1485](#)].
- [28] M. Fairbairn, P. Scott, and J. Edsjö, *The zero age main sequence of WIMP burners*, *Phys. Rev. D* **77** (2008) 047301, [[arXiv:0710.3396](#)].
- [29] P. Scott, J. Edsjö, and M. Fairbairn, *Low mass stellar evolution with WIMP capture and annihilation*, in *Dark Matter in Astroparticle and Particle Physics: Dark 2007* (H. K. Klapdor-Kleingrothaus and G. F. Lewis, eds.), World Scientific, Singapore (2008) 387–392, [[arXiv:0711.0991](#)].
- [30] F. Iocco, *Dark Matter Capture and Annihilation on the First Stars: Preliminary Estimates*, *ApJ* **677** (2008) L1–L4, [[arXiv:0802.0941](#)].
- [31] F. Iocco, A. Bressan, *et. al.*, *Dark matter annihilation effects on the first stars*, *MNRAS* **390** (2008) 1655–1669, [[arXiv:0805.4016](#)].
- [32] P. Scott, M. Fairbairn, and J. Edsjö, *Dark stars at the Galactic Centre - the main sequence*, *MNRAS* **394** (2009) 82–104, [[arXiv:0809.1871](#)].
- [33] J. Casanellas and I. Lopes, *The Formation and Evolution of Young Low-mass Stars within Halos with High Concentration of Dark Matter Particles*, *ApJ* **705** (2009) 135–143, [[arXiv:0909.1971](#)].
- [34] E. Ripamonti, F. Iocco, *et. al.*, *First star formation with dark matter annihilation*, *MNRAS* **406** (2010) 2605–2615, [[arXiv:1003.0676](#)].
- [35] R. L. Gilliland, J. Faulkner, W. H. Press, and D. N. Spergel, *Solar models with energy transport by weakly interacting particles*, *ApJ* **306** (1986) 703–709.
- [36] A. Renzini, *Effects of cosmions in the sun and in globular cluster stars*, *A&A* **171** (1987) 121.

- [37] D. N. Spergel and J. Faulkner, *Weakly interacting, massive particles in horizontal-branch stars*, *ApJ* **331** (1988) L21–L24.
- [38] J. Faulkner and F. J. Swenson, *Main-sequence evolution with efficient central energy transport*, *ApJ* **329** (1988) L47–L50.
- [39] A. Bouquet, J. Kaplan, and F. Martin, *Weakly interacting massive particles and stellar structure*, *A&A* **222** (1989) 103–116.
- [40] A. Bouquet and P. Salati, *Dark matter and the suppression of stellar core convection*, *ApJ* **346** (1989) 284–288.
- [41] P. Salati, *Dark matter particles as inhibitors of the solar core pulsations*, *ApJ* **348** (1990) 738–747.
- [42] D. Dearborn, G. Raffelt, P. Salati, J. Silk, and A. Bouquet, *Dark matter and the age of globular clusters*, *Nature* **343** (1990) 347.
- [43] D. Dearborn, G. Raffelt, P. Salati, J. Silk, and A. Bouquet, *Dark matter and thermal pulses in horizontal-branch stars*, *ApJ* **354** (1990) 568–582.
- [44] Y. Giraud-Heraud, J. Kaplan, F. M. de Volnay, C. Tao, and S. Turck-Chieze, *WIMPs and solar evolution code*, *Sol. Phys.* **128** (1990) 21–33.
- [45] J. Christensen-Dalsgaard, *Solar models with enhanced energy transport in the core*, *ApJ* **385** (1992) 354–362.
- [46] J. Faulkner and F. J. Swenson, *Sub-giant branch evolution and efficient central energy transport*, *ApJ* **411** (1993) 200–206.
- [47] F. Iocco, M. Taoso, F. Leclercq, and G. Meynet, *Main Sequence Stars with Asymmetric Dark Matter*, *Phys. Rev. Lett.* **108** (2012) 061301, [[arXiv:1201.5387](#)].
- [48] I. P. Lopes, J. Silk, and S. H. Hansen, *Helioseismology as a new constraint on supersymmetric dark matter*, *MNRAS* **331** (2002) 361–368, [[astro-ph/0111530](#)].
- [49] I. P. Lopes, G. Bertone, and J. Silk, *Solar seismic model as a new constraint on supersymmetric dark matter*, *MNRAS* **337** (2002) 1179–1184, [[astro-ph/0205066](#)].
- [50] A. Bottino, G. Fiorentini, *et. al.*, *Does solar physics provide constraints to weakly interacting massive particles?*, *Phys. Rev. D* **66** (2002) 053005, [[hep-ph/0206211](#)].
- [51] M. T. Frandsen and S. Sarkar, *Asymmetric Dark Matter and the Sun*, *Phys. Rev. Lett.* **105** (2010) 011301, [[arXiv:1003.4505](#)].
- [52] M. Taoso, F. Iocco, G. Meynet, G. Bertone, and P. Eggenberger, *Effect of low mass dark matter particles on the Sun*, *Phys. Rev. D* **82** (2010) 083509, [[arXiv:1005.5711](#)].
- [53] D. T. Cumberbatch, J. A. Guzik, J. Silk, L. S. Watson, and S. M. West, *Light WIMPs in the Sun: Constraints from helioseismology*, *Phys. Rev. D* **82** (2010) 103503, [[arXiv:1005.5102](#)].
- [54] I. Lopes and J. Silk, *Solar Constraints on Asymmetric Dark Matter*, *ApJ* **757** (2012) 130, [[arXiv:1209.3631](#)].
- [55] J. Casanellas and I. Lopes, *First Asteroseismic Limits on the Nature of Dark Matter*, *ApJ* **765** (2013) L21, [[arXiv:1212.2985](#)].
- [56] I. Lopes, K. Kadota, and J. Silk, *Constraint on Light Dipole Dark Matter from Helioseismology*, [[arXiv:1310.0673](#)].
- [57] C. Allende Prieto, D. L. Lambert, and M. Asplund, *The Forbidden Abundance of Oxygen in the Sun*, *ApJ* **556** (2001) L63–L66, [[astro-ph/0106360](#)].
- [58] C. Allende Prieto, D. L. Lambert, and M. Asplund, *A Reappraisal of the Solar Photospheric C/O Ratio*, *ApJ* **573** (2002) L137–L140, [[astro-ph/0206089](#)].
- [59] M. Asplund, N. Grevesse, A. J. Sauval, C. Allende Prieto, and D. Kiselman, *Line formation in solar granulation. IV. [O I], O I and OH lines and the photospheric O abundance*, *A&A* **417** (2004) 751–768, [[astro-ph/0312290](#)].
- [60] M. Asplund, N. Grevesse, A. J. Sauval, C. Allende Prieto, and R. Blomme, *Line formation in solar granulation. VI. [C I], C I, CH and C<sub>2</sub> lines and the photospheric C abundance*, *A&A* **431** (2005) 693–705, [[astro-ph/0410681](#)].
- [61] M. Asplund, N. Grevesse, and A. J. Sauval, *The Solar Chemical Composition*, in *Cosmic Abundances as Records of Stellar Evolution and Nucleosynthesis* (T. G. Barnes III and F. N. Bash, eds.), Astron. Soc. Pac., San Francisco, *ASP Conf. Ser.* **336** (2005) 25.
- [62] P. Scott, M. Asplund, N. Grevesse, and A. J. Sauval, *Line formation in solar granulation. VII. CO lines and the solar C and O isotopic abundances*, *A&A* **456** (2006) 675–688, [[astro-ph/0605116](#)].
- [63] J. Meléndez and M. Asplund, *Another forbidden solar oxygen abundance: the [O I] 5577 Å line*, *A&A* **490** (2008) 817–821, [[arXiv:0808.2796](#)].
- [64] P. Scott, M. Asplund, N. Grevesse, and A. J. Sauval, *On the Solar Nickel and Oxygen Abundances*, *ApJ* **691** (2009) L119–L122, [[arXiv:0811.0815](#)].
- [65] M. Asplund, N. Grevesse, A. J. Sauval, and P. Scott, *The chemical composition of the Sun*, *ARA&A* **47** (2009) 481–522, [[arXiv:0909.0948](#)].
- [66] J. N. Bahcall, S. Basu, M. Pinsonneault, and A. M. Serenelli, *Helioseismological implications of recent solar abundance determinations*, *ApJ* **618** (2005) 1049–1056, [[astro-ph/0407060](#)].
- [67] S. Basu and H. Antia, *Constraining solar abundances using helioseismology*, *ApJ* **606** (2004) L85, [[astro-ph/0403485](#)].
- [68] J. N. Bahcall, A. M. Serenelli, and S. Basu, *10,000 Standard Solar Models: A Monte Carlo Simulation*, *ApJS* **165** (2006) 400–431, [[astro-ph/0511337](#)].
- [69] W. M. Yang and S. L. Bi, *Solar Models with Revised Abundances and Opacities*, *ApJ* **658** (2007) L67–L70, [[arXiv:0805.3644](#)].
- [70] S. Basu and H. M. Antia, *Helioseismology and solar abundances*, *Phys. Rep.* **457** (2008) 217–283, [[arXiv:0711.4590](#)].
- [71] A. Serenelli, S. Basu, J. W. Ferguson, and M. Asplund, *New Solar Composition: The Problem With Solar Models Revisited*, *ApJ* **705** (2009) L123–L127, [[arXiv:0909.2668](#)].
- [72] J. N. Bahcall, A. M. Serenelli, and S. Basu, *New Solar Opacities, Abundances, Helioseismology, and Neutrino Fluxes*, *ApJ* **621** (2005) L85–L88, [[astro-ph/0412440](#)].
- [73] N. R. Badnell, M. A. Bautista, *et. al.*, *Updated opacities from the Opacity Project*, *MNRAS* **360** (2005) 458–464, [[astro-ph/0410744](#)].
- [74] D. Arnett, C. Meakin, and P. A. Young, *The Lambert Problem*, in *Cosmic Abundances as Records of Stellar Evolution and Nucleosynthesis* (T. G. Barnes, III and F. N. Bash, eds.) **336** (2005) 235.
- [75] C. Charbonnel and S. Talon, *Influence of Gravity Waves on the Internal Rotation and Li Abundance of Solar-Type Stars*, *Science* **309** (2005) 2189–2191,

- [astro-ph/0511265].
- [76] J. A. Guzik, L. S. Watson, and A. N. Cox, *Can Enhanced Diffusion Improve Helioseismic Agreement for Solar Models with Revised Abundances?*, *ApJ* **627** (2005) 1049–1056, [astro-ph/0502364].
- [77] M. Castro, S. Vauclair, and O. Richard, *Low abundances of heavy elements in the solar outer layers: comparisons of solar models with helioseismic inversions*, *A&A* **463** (2007) 755–758, [astro-ph/0611619].
- [78] J. Christensen-Dalsgaard, M. P. di Mauro, G. Houdek, and F. Pijpers, *On the opacity change required to compensate for the revised solar composition*, *A&A* **494** (2009) 205–208, [arXiv:0811.1001].
- [79] J. A. Guzik and K. Mussack, *Exploring Mass Loss, Low-Z Accretion, and Convective Overshoot in Solar Models to Mitigate the Solar Abundance Problem*, *ApJ* **713** (2010) 1108–1119, [arXiv:1001.0648].
- [80] A. M. Serenelli, W. C. Haxton, and C. Peña-Garay, *Solar Models with Accretion. I. Application to the Solar Abundance Problem*, *ApJ* **743** (2011) 24, [arXiv:1104.1639].
- [81] A. C. Vincent, P. Scott, and R. Trampedach, *Light bosons in the photosphere and the solar abundance problem*, *MNRAS* **432** (2013) 3332–3339, [arXiv:1206.4315].
- [82] DAMA Collaboration: R. Bernabei, P. Belli, *et al.*, *First results from DAMA/LIBRA and the combined results with DAMA/NaI*, *Eur. Phys. J. C* (2008) 167, [arXiv:0804.2741].
- [83] CoGeNT Collaboration: C. E. Aalseth, P. S. Barbeau, *et al.*, *Search for an Annual Modulation in a p-Type Point Contact Germanium Dark Matter Detector*, *Phys. Rev. Lett.* **107** (2011) 141301, [arXiv:1106.0650].
- [84] CRESST Collaboration: G. Angloher, M. Bauer, *et al.*, *Results from 730 kg days of the CRESST-II Dark Matter search*, *Eur. Phys. J. C* **72** (2012) 1971, [arXiv:1109.0702].
- [85] CDMS Collaboration: R. Agnese *et al.*, *Dark Matter Search Results Using the Silicon Detectors of CDMS II*, *Phys. Rev. Lett.* (2013) in press, [arXiv:1304.4279].
- [86] A. L. Fitzpatrick, W. Haxton, E. Katz, N. Lubbers, and Y. Xu, *The effective field theory of dark matter direct detection*, *JCAP* **2** (2013) 4, [arXiv:1203.3542].
- [87] J. Kumar and D. Marfatia, *Matrix element analyses of dark matter scattering and annihilation*, *Phys. Rev. D* **88** (2013) 014035, [arXiv:1305.1611].
- [88] LUX Collaboration: D. Akerib *et al.*, *First results from the LUX dark matter experiment at the Sanford Underground Research Facility*, [arXiv:1310.8214].
- [89] XENON10 Collaboration: J. Angle *et al.*, *A search for light dark matter in XENON10 data*, *Phys. Rev. Lett.* **107** (2011) 051301, [arXiv:1104.3088].
- [90] XENON100 Collaboration: E. Aprile, M. Alfonsi, *et al.*, *Dark Matter Results from 225 Live Days of XENON100 Data*, *Phys. Rev. Lett.* **109** (2012) 181301, [arXiv:1207.5988].
- [91] COUPP Collaboration: E. Behnke, J. Behnke, *et al.*, *First dark matter search results from a 4-kg CF<sub>3</sub>I bubble chamber operated in a deep underground site*, *Phys. Rev. D* **86** (2012) 052001, [arXiv:1204.3094].
- [92] SIMPLE Collaboration: M. Felizardo, T. A. Girard, *et al.*, *Final Analysis and Results of the Phase II SIMPLE Dark Matter Search*, *Phys. Rev. Lett.* **108** (2012) 201302, [arXiv:1106.3014].
- [93] N. Bozorgnia, J. Herrero-Garcia, T. Schwetz, and J. Zupan, *Halo-independent methods for inelastic dark matter scattering*, *JCAP* **7** (2013) 49, [arXiv:1305.3575].
- [94] Y.-Y. Mao, L. E. Strigari, and R. H. Wechsler, *Connecting Direct Dark Matter Detection Experiments to Cosmologically Motivated Halo Models*, [arXiv:1304.6401].
- [95] E. Massó, S. Mohanty, and S. Rao, *Dipolar dark matter*, *Phys. Rev. D* **80** (2009) 036009, [arXiv:0906.1979].
- [96] B. Feldstein, A. L. Fitzpatrick, and E. Katz, *Form Factor Dark Matter*, *JCAP* **1001** (2010) 020, [arXiv:0908.2991].
- [97] S. Chang, A. Pierce, and N. Weiner, *Momentum Dependent Dark Matter Scattering*, *JCAP* **1001** (2010) 006, [arXiv:0908.3192].
- [98] B. Feldstein, A. L. Fitzpatrick, E. Katz, and B. Tweedie, *A simple explanation for DAMA with moderate channeling*, *JCAP* **3** (2010) 29, [arXiv:0910.0007].
- [99] S. Chang, J. Liu, A. Pierce, N. Weiner, and I. Yavin, *CoGeNT interpretations*, *JCAP* **8** (2010) 18, [arXiv:1004.0697].
- [100] H. An, S.-L. Chen, R. N. Mohapatra, S. Nussinov, and Y. Zhang, *Energy dependence of direct detection cross section for asymmetric mirror dark matter*, *Phys. Rev. D* **82** (2010) 023533, [arXiv:1004.3296].
- [101] S. Chang, N. Weiner, and I. Yavin, *Magnetic Inelastic Dark Matter*, *Phys. Rev. D* **82** (2010) 125011, [arXiv:1007.4200].
- [102] V. Barger, W.-Y. Keung, and D. Marfatia, *Electromagnetic properties of dark matter: Dipole moments and charge form factor*, *Physics Letters B* **696** (2011) 74–78, [arXiv:1007.4345].
- [103] A. L. Fitzpatrick and K. M. Zurek, *Dark moments and the DAMA-CoGeNT puzzle*, *Phys. Rev. D* **82** (2010) 075004, [arXiv:1007.5325].
- [104] M. T. Frandsen, F. Kahlhoefer, C. McCabe, S. Sarkar, and K. Schmidt-Hoberg, *The unbearable lightness of being: CDMS versus XENON*, *JCAP* **7** (2013) 23, [arXiv:1304.6066].
- [105] M. Pospelov and T. ter Veldhuis, *Direct and indirect limits on the electro-magnetic form factors of WIMPs*, *Phys. Lett. B* **480** (2000) 181–186, [hep-ph/0003010].
- [106] K. Sigurdson, M. Doran, A. Kurylov, R. R. Caldwell, and M. Kamionkowski, *Dark-matter electric and magnetic dipole moments*, *Phys. Rev. D* **70** (2004) 083501, [astro-ph/0406355].
- [107] E. Del Nobile, G. Gelmini, P. Gondolo, and J.-H. Huh, *Generalized halo independent comparison of direct dark matter detection data*, *JCAP* **10** (2013) 48, [arXiv:1306.5273].
- [108] A. Sommerfeld, *Über die Beugung und Bremsung der Elektronen*, *Ann. Phys.* **403** (1931) 257–330.
- [109] J. Hisano, S. Matsumoto, M. M. Nojiri, and O. Saito, *Nonperturbative effect on dark matter annihilation and gamma ray signature from the galactic center*, *Phys. Rev. D* **71** (2005) 063528, [hep-ph/0412403].
- [110] N. Arkani-Hamed, D. P. Finkbeiner, T. R. Slatyer, and N. Weiner, *A theory of dark matter*, *Phys. Rev. D* **79**

- (2009) 015014, [[arXiv:0810.0713](#)].
- [111] P. S. Krstić and D. R. Schultz, *Consistent definitions for, and relationships among, cross sections for elastic scattering of hydrogen ions, atoms, and molecules*, *Phys. Rev. A* **60** (1999) 2118–2130.
- [112] S. Tulin, H.-B. Yu, and K. M. Zurek, *Beyond collisionless dark matter: Particle physics dynamics for dark matter halo structure*, *Phys. Rev. D* **87** (2013) 115007, [[arXiv:1302.3898](#)].
- [113] A. Gould and G. Raffelt, *Cosmion energy transfer in stars - The Knudsen limit*, *ApJ* **352** (1990) 669–680.
- [114] A. C. Vincent, A. Serenelli, and P. Scott *in prep.*

TABLE II. Tabulated values of  $\alpha$  (left) and  $\log_{10} \kappa$  (right) for the different cross-sections studied in this paper, at selected logarithmically-spaced values of  $\mu = m_\chi/m_{\text{nuc}}$ .

$\mu \backslash \sigma \propto$	<i>const.</i>	$v^{-2}$	$v^2$	$v^4$	$q^{-2}$	$q^2$	$q^4$	<i>const.</i>	$v^{-2}$	$v^2$	$v^4$	$q^{-2}$	$q^2$	$q^4$
	$\alpha$							$\log_{10} \kappa$						
0.0100	2.0049	2.9994	1.0721	0.4117	2.9990	1.0588	0.3789	0.0317	0.5139	-0.3024	-0.4960	0.5139	-0.4225	-0.6543
0.0120	2.0059	2.9993	1.0814	0.4331	2.9988	1.0665	0.3981	0.0317	0.5148	-0.3070	-0.5107	0.5148	-0.4262	-0.6675
0.0145	2.0071	2.9993	1.0920	0.4562	2.9987	1.0754	0.4189	0.0323	0.5167	-0.3114	-0.5264	0.5167	-0.4298	-0.6817
0.0175	2.0085	2.9992	1.1040	0.4810	2.9985	1.0855	0.4410	0.0333	0.5190	-0.3163	-0.5433	0.5190	-0.4339	-0.6971
0.0210	2.0102	2.9990	1.1173	0.5075	2.9983	1.0967	0.4647	0.0345	0.5218	-0.3217	-0.5617	0.5218	-0.4384	-0.7139
0.0254	2.0122	2.9988	1.1320	0.5358	2.9980	1.1091	0.4900	0.0359	0.5251	-0.3277	-0.5818	0.5251	-0.4434	-0.7322
0.0305	2.0146	2.9985	1.1483	0.5659	2.9977	1.1230	0.5169	0.0376	0.5290	-0.3343	-0.6036	0.5290	-0.4489	-0.7522
0.0368	2.0176	2.9980	1.1662	0.5980	2.9973	1.1383	0.5456	0.0396	0.5336	-0.3415	-0.6273	0.5336	-0.4550	-0.7741
0.0443	2.0211	2.9973	1.1860	0.6321	2.9968	1.1552	0.5761	0.0419	0.5390	-0.3494	-0.6530	0.5390	-0.4617	-0.7979
0.0534	2.0253	2.9962	1.2077	0.6684	2.9961	1.1739	0.6085	0.0446	0.5452	-0.3581	-0.6810	0.5452	-0.4691	-0.8239
0.0643	2.0304	2.9947	1.2315	0.7069	2.9953	1.1945	0.6429	0.0477	0.5524	-0.3676	-0.7113	0.5524	-0.4771	-0.8522
0.0774	2.0365	2.9926	1.2575	0.7477	2.9943	1.2172	0.6792	0.0513	0.5605	-0.3779	-0.7441	0.5605	-0.4859	-0.8830
0.0933	2.0438	2.9894	1.2860	0.7908	2.9929	1.2421	0.7176	0.0553	0.5698	-0.3892	-0.7796	0.5698	-0.4955	-0.9164
0.1123	2.0525	2.9849	1.3172	0.8365	2.9912	1.2696	0.7582	0.0597	0.5801	-0.4014	-0.8178	0.5801	-0.5060	-0.9526
0.1353	2.0630	2.9787	1.3512	0.8847	2.9889	1.2999	0.8009	0.0644	0.5915	-0.4146	-0.8591	0.5915	-0.5173	-0.9917
0.1630	2.0755	2.9699	1.3885	0.9355	2.9859	1.3334	0.8458	0.0693	0.6038	-0.4290	-0.9033	0.6038	-0.5297	-1.0339
0.1963	2.0904	2.9581	1.4293	0.9893	2.9820	1.3705	0.8932	0.0742	0.6170	-0.4447	-0.9507	0.6170	-0.5433	-1.0792
0.2364	2.1078	2.9423	1.4741	1.0462	2.9768	1.4117	0.9431	0.0789	0.6308	-0.4619	-1.0014	0.6308	-0.5582	-1.1277
0.2848	2.1282	2.9222	1.5232	1.1066	2.9702	1.4576	0.9960	0.0829	0.6450	-0.4808	-1.0554	0.6450	-0.5747	-1.1794
0.3430	2.1514	2.8972	1.5771	1.1710	2.9616	1.5091	1.0523	0.0860	0.6594	-0.5017	-1.1129	0.6594	-0.5932	-1.2344
0.4132	2.1774	2.8677	1.6362	1.2401	2.9508	1.5667	1.1130	0.0876	0.6738	-0.5253	-1.1739	0.6738	-0.6142	-1.2927
0.4977	2.2058	2.8342	1.7005	1.3146	2.9373	1.6311	1.1794	0.0875	0.6883	-0.5519	-1.2390	0.6883	-0.6386	-1.3544
0.5995	2.2359	2.7982	1.7698	1.3955	2.9210	1.7023	1.2534	0.0855	0.7033	-0.5824	-1.3085	0.7033	-0.6671	-1.4201
0.7221	2.2667	2.7611	1.8431	1.4835	2.9016	1.7797	1.3370	0.0816	0.7192	-0.6173	-1.3833	0.7192	-0.7006	-1.4906
0.8697	2.2971	2.7247	1.9186	1.5785	2.8794	1.8615	1.4321	0.0763	0.7373	-0.6571	-1.4645	0.7373	-0.7399	-1.5676
1.0476	2.3261	2.6906	1.9941	1.6793	2.8544	1.9449	1.5390	0.0702	0.7586	-0.7020	-1.5530	0.7586	-0.7853	-1.6527
1.2619	2.3528	2.6596	2.0669	1.7831	2.8274	2.0264	1.6557	0.0641	0.7845	-0.7516	-1.6497	0.7845	-0.8366	-1.7477
1.5199	2.3767	2.6324	2.1345	1.8859	2.7989	2.1027	1.7770	0.0589	0.8160	-0.8052	-1.7547	0.8160	-0.8929	-1.8536
1.8307	2.3975	2.6090	2.1950	1.9831	2.7697	2.1710	1.8957	0.0556	0.8542	-0.8615	-1.8674	0.8542	-0.9528	-1.9700
2.2051	2.4153	2.5894	2.2477	2.0711	2.7407	2.2302	2.0049	0.0548	0.8997	-0.9193	-1.9863	0.8997	-1.0146	-2.0953
2.6561	2.4302	2.5731	2.2923	2.1476	2.7125	2.2798	2.0999	0.0572	0.9528	-0.9773	-2.1093	0.9528	-1.0766	-2.2265
3.1993	2.4426	2.5597	2.3295	2.2119	2.6858	2.3208	2.1788	0.0631	1.0133	-1.0345	-2.2346	1.0133	-1.1376	-2.3606
3.8535	2.4528	2.5487	2.3601	2.2648	2.6610	2.3540	2.2423	0.0727	1.0812	-1.0903	-2.3604	1.0812	-1.1968	-2.4948
4.6416	2.4612	2.5397	2.3851	2.3079	2.6384	2.3810	2.2928	0.0857	1.1559	-1.1444	-2.4857	1.1559	-1.2539	-2.6276
5.5908	2.4681	2.5324	2.4056	2.3428	2.6181	2.4027	2.3326	0.1022	1.2369	-1.1967	-2.6102	1.2369	-1.3087	-2.7582
6.7342	2.4737	2.5265	2.4223	2.3710	2.6002	2.4204	2.3641	0.1218	1.3236	-1.2472	-2.7336	1.3236	-1.3613	-2.8867
8.1113	2.4783	2.5216	2.4360	2.3939	2.5844	2.4346	2.3892	0.1444	1.4154	-1.2961	-2.8560	1.4154	-1.4121	-3.0133
9.7701	2.4822	2.5177	2.4472	2.4126	2.5708	2.4463	2.4094	0.1695	1.5117	-1.3437	-2.9779	1.5117	-1.4611	-3.1384
11.768	2.4854	2.5145	2.4564	2.4278	2.5590	2.4558	2.4256	0.1968	1.6119	-1.3901	-3.0992	1.6119	-1.5088	-3.2624
14.175	2.4881	2.5118	2.4640	2.4404	2.5490	2.4635	2.4389	0.2262	1.7156	-1.4355	-3.2201	1.7156	-1.5552	-3.3855
17.074	2.4903	2.5096	2.4703	2.4507	2.5404	2.4699	2.4496	0.2573	1.8224	-1.4800	-3.3408	1.8224	-1.6006	-3.5081
20.565	2.4920	2.5077	2.4755	2.4592	2.5332	2.4752	2.4584	0.2898	1.9321	-1.5239	-3.4615	1.9321	-1.6453	-3.6303
24.771	2.4934	2.5060	2.4798	2.4663	2.5271	2.4795	2.4657	0.3237	2.0444	-1.5671	-3.5820	2.0444	-1.6891	-3.7521
29.837	2.4946	2.5046	2.4833	2.4721	2.5220	2.4831	2.4716	0.3586	2.1594	-1.6099	-3.7027	2.1594	-1.7325	-3.8738
35.938	2.4956	2.5034	2.4862	2.4769	2.5177	2.4860	2.4765	0.3946	2.2771	-1.6522	-3.8233	2.2771	-1.7753	-3.9953
43.288	2.4964	2.5023	2.4886	2.4809	2.5141	2.4884	2.4806	0.4315	2.3978	-1.6941	-3.9439	2.3978	-1.8176	-4.1166
52.140	2.4972	2.5012	2.4906	2.4843	2.5111	2.4904	2.4839	0.4690	2.5224	-1.7357	-4.0646	2.5224	-1.8597	-4.2380
62.803	2.4978	2.5001	2.4924	2.4870	2.5085	2.4921	2.4867	0.5073	2.6519	-1.7770	-4.1853	2.6519	-1.9015	-4.3593
75.646	2.4984	2.4990	2.4939	2.4894	2.5064	2.4935	2.4890	0.5462	2.7884	-1.8181	-4.3060	2.7884	-1.9431	-4.4806
91.116	2.4989	2.4976	2.4952	2.4914	2.5045	2.4946	2.4909	0.5859	2.9354	-1.8589	-4.4267	2.9354	-1.9844	-4.6018
100.00	2.4991	2.4969	2.4957	2.4923	2.5037	2.4951	2.4917	0.6061	3.0146	-1.8792	-4.4870	3.0146	-2.0050	-4.6624